



USDOT Tier 1 University Transportation Center Final Report

NURail Project No. #NURail2012-MTU-R04

**Cross-Infrastructure Learnings for Alternative Bridge
System Designs – A Case Study on the Hybrid Composite
Bridge System**

By

Devin Harris
Assistant Professor Civil and Environmental Engineering
University of Virginia
dharris@virginia.edu

John Civitillo
Former Masters Student of Civil and Environmental Engineering
University of Virginia

Amir Gheitasi
Post-Doctoral Research Associate Civil and Environmental Engineering
University of Virginia

DISCLAIMER

Funding for this research was provided by the NURail Center, University of Illinois at Urbana - Champaign under Grant No. DTRT12-G-UTC18 of the U.S. Department of Transportation, Office of the Assistant Secretary for Research & Technology (OST-R), University Transportation Centers Program. The contents of this report reflect the views of the authors, who are responsible for the facts and the accuracy of the information presented herein. This document is disseminated under the sponsorship of the U.S. Department of Transportation's University Transportation Centers Program, in the interest of information exchange. The U.S. Government assumes no liability for the contents or use thereof.

Abstract

The hybrid composite beam (HCB) technology has been presented as a system for short and medium span beam bridges as an alternative to traditional materials such as concrete and steel. A HCB consists of a concrete tied arch encased in a fiber-reinforced polymer (FRP) shell. When compared to traditional materials, the HCB system is lighter in weight, which allows for multiple members to be transported on a single truck and smaller cranes to be used during construction, and even reuse of existing substructures. In addition, the protective nature of the FRP outer shell provides additional resistance to corrosion for the reinforcement internal to the system, potentially offering an extended lifespan over conventional girders. Similar to other beam-type bridges for highways, the HCB system is made composite with a conventionally reinforced concrete deck.

The investigation presented herein was limited to the evaluation of the in-service performance of a HCB bridge constructed in Virginia by the Virginia Department of Transportation. This bridge was evaluated for highway applications, but provided critical information related to the overall system performance that is also relevant to railroad and transit applications. These performance characteristics include lateral load distribution, dynamic load allowance and internal load sharing mechanisms inherent to the HCB design. Results from a live load testing program are synthesized in this report along with considerations for future railroad applications.



USDOT Tier 1 University Transportation Center Final Report

TECHNICAL SUMMARY

NURail Project No. NURail2012-MTU-R04

Final Report April 30, 2015

Title

Cross-Infrastructure Learnings for Alternative Bridge System Designs – A Case Study on the Hybrid Composite Bridge System

Introduction

A relatively new technology in the field of structural engineering, hybrid composite beams (HCB), have been deployed in bridges as an alternative to traditional materials such as concrete and steel. As a brief descriptor, the HCB is essentially a concrete tied arch encased in a fiber-reinforced polymer (FRP) shell. When compared to steel and concrete, the HCB system is lighter in weight, which allows for multiple members to be transported on a single truck and smaller cranes to be used during construction, and even reuse of existing substructures. For railroad applications, these characteristics may be ideal for remote areas or even rapid replacement applications. In addition, the protective nature of the FRP outer shell provides additional resistance to corrosion for the reinforcement internal to the system, potentially offering an extended lifespan over conventional girders. Similar to other beam type bridges for highways, the HCB system can be made composite with a conventionally reinforced concrete deck.

The bridge application studied in this investigation leveraged an implementation application by the Virginia Department of Transportation, which included the design and construction of a HCB bridge in Colonial Beach, Virginia. The design proposed the construction of an HCB Bridge System as a replacement for the existing bridge that crossed Tides Mill Stream along Route 205 in Colonial Beach, VA. The existing bridge structure was a 44 ft span simply-supported concrete girder bridge with 45° skew and served as a primary connector route for the Colonial Beach community. The primary goal of the investigation was to gain a better understanding of the system behavior including how the loads are transmitted, both at the system and element levels, and also an understanding of dynamic characteristics of the system. This report includes a synthesis of the live load testing program of this bridge, but additional details are available in the final VCTIR Report available at: <http://vtrc.virginiadot.org/AllPubs.aspx>.

Purpose and Scope

The focus of this study was on the characterization of the in-service structural behavior of the Hybrid Composite Beam bridge system used on the structure constructed by VDOT on Route 205 over the Tides Mill Stream in Colonial Beach, VA. The in-service evaluation was intended to provide details on the structural behavior characteristics of this system, which could be extended to railroad applications.

The goal of the investigation was to use traditional live-load testing strategies to validate the design assumptions used in the construction of this bridge and provide corroboration with the results from a previous experimental program at Virginia Tech. The behavior characteristics of particular interest included the flexural lateral load distribution behavior, the element load sharing behavior, and the dynamic load amplification of this skewed HCB application.

It should be noted that the original project objectives included the development of a comprehensive finite element model of the HCB system which could then be used as a parametric investigation tool; however, the model development proved to be more challenging than anticipated due to the complex geometry and the uncertainty in the composite element behavior determined during the live load testing program. As a result, this study includes only the findings related to the in-service evaluation of the HCB system.

Literature Review

The idea of hybrid-composite beam technology made its debut in a bridge construction application as a prototype railroad bridge in 2007 (Hillman 2008; Otter and Doe 2009; Otter and Tunna 2011), making it extremely young for a civil engineering technology. Since the prototype testing at the Transportation Technology Center, Inc. (TTCI) in Pueblo, Colorado, HCBs have been used in another railroad project in Colorado as well as highway projects in Illinois, New Jersey, Maine, and several projects in Missouri. Many of these HCB applications have not included in-service evaluation or field-testing of the constructed bridges. Accordingly, with the HCB being a relatively new technology (Hillman 2003), limited technical literature is available. While HCB is gaining acceptance as a viable design solution and being used in more applications, many projects do not involve accompanying research, or the data is yet to be published.

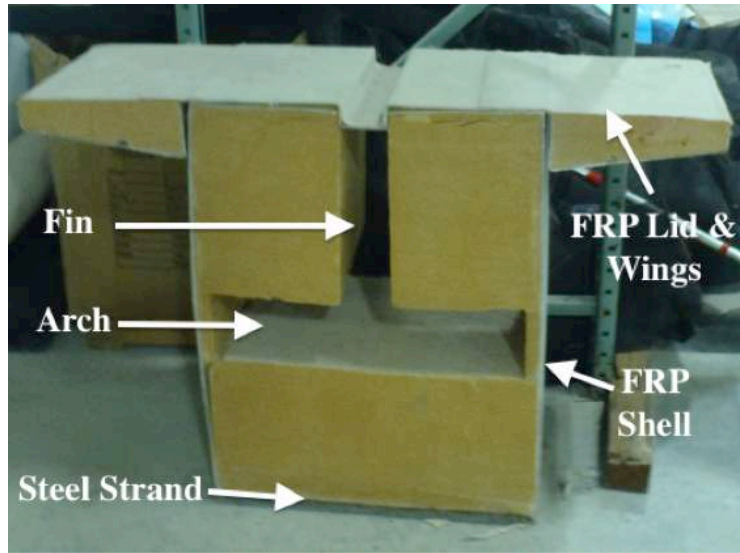
HCB Background, Design, and Theoretical Behavior

Materials and Configuration

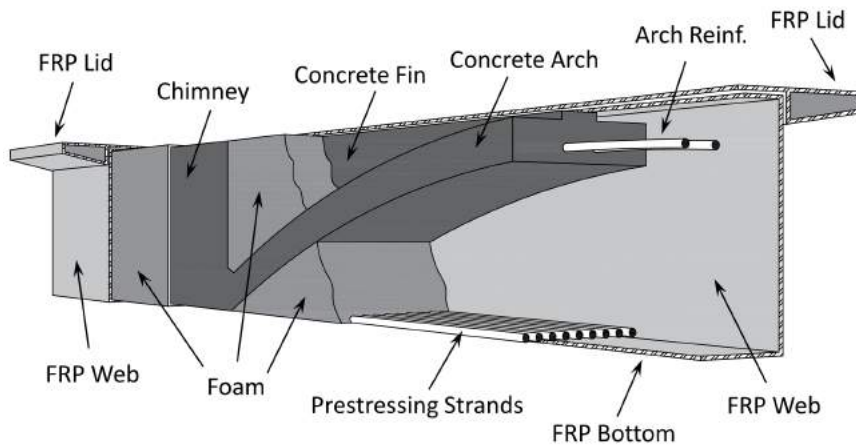
As highlighted in the previous section, the HCB system at its core can be described simplistically as a tied concrete arch encased in a FRP shell. A single beam consists of a parabolic concrete arch tied in the tension zone by steel, carbon fiber, or glass fiber prestressing strand. Under bending, the beam distributes loads from the top of the beam through axial compression of the arch down to the supports, where the tension strands restrain the supports. The entire arch system is contained within a glass fiber-reinforced polymer (FRP) box shell that protects the main load carrying

components and contributes additional shear resistance. Figure 1 provides a visual representation of the orientation of each of the aforementioned components.

For the FRP shell or box, a quad-weave fiber fabric is used to avoid custom alignment of fiber orientations for each application. In this fabric, 45 percent of the fibers are orientated in the longitudinal direction, while 25 percent run in both a positive and negative 45-degree orientation from the longitudinal axis. The remaining 30 percent of the fibers run in the direction perpendicular to the length of the beam (Hillman 2003). During fabrication of the beam, several layers of the fiberglass fabric are laid in the box formwork. The tension zone reinforcement is laid in the base of the beam formwork and covered with a single additional fiberglass sheet prior to the resin infusion process. Options for the tension reinforcement include carbon fiber, glass fiber prestressing strands, as well as traditional steel strands and a welded steel wire mesh. While each is a valid option, steel remains the most cost effective (Hillman 2003). The core formwork, cut of polyisocyanurate foam, is laid in the mold next, filling the void space of the box while retaining the arch-shaped formwork for the concrete to be filled in the beam at a later time. The height of the voided concrete formwork varies parabolically over the length of the beam to create the arch shape.



(a)



(b)

Figure 1 - Hybrid Composite Beam (a) cross-section and (b) isometric system

The shell is then infused with a vinyl ester resin through a closed-mold vacuum-assisted resin transfer method (VARTM), which upon infusion creates a composite unit of FRP, steel and foam (Hillman and Otter 2008). During this process, the foam supports the beam shape during the vacuum application, and maintains the arch profile. While the foam alone is not structurally significant, it does offer some lateral stability to the beam, improves the elastic buckling capacity of the FRP webs, and helps to distribute the load to the rest of the beam beneath the concrete arch (Hillman 2003). The companion study by Virginia Tech confirmed this contribution, but also noted that the foam is critical for helping the development of the shear resistance through tension field action in the webs.

The FRP lid and wings are manufactured separately from the rest of the beam, but glued together prior to placement of the arch concrete. Inclined shear connectors,

consisting of conventional steel rebar, are inserted through holes drilled in the middle of the lid and fed down through the vertical concrete 'fin' (Figure 1) to the concrete arch and serve to enforce composite action between the HCB and a conventionally cast reinforced concrete deck. Once the shear connectors are in place, a highly workable concrete mixture, typically self-consolidating concrete (SCC) is fed into the beam to fill the voided conduits. The concrete is vibrated to ensure that all void spaces are filled entirely.

Design

The geometry of these beams is complicated when compared to a conventionally reinforced concrete beam, but the current design methodology includes simplifying design assumptions that allow for use of traditional beam theory (Hillman 2003). These include assumptions that all materials behave in a linear elastic manner under service loads, and that plane sections remain plane during flexure. A transformed section approach is used, converting steel and concrete sections to equivalent FRP sections. Section properties including centroid and moment of inertia are generated for the tenth points along the beam's length. Design loading values are drawn from AASHTO, including distribution factors, multiple presence factors, and dynamic load amplifications for an HL-93 design truck, and applied at the tenth points to determine the controlling moment and shears (Hillman, 2011).

The strength limit state for flexure is checked by a comparison of the strains at mid-span to ultimate strain values for each material. The shear strength is limited to the allowable shear stress capacity of the FRP webs, which was defined as 7.5 ksi. Due to the inclined profile of the arch in compression, the vertical component of the axial load is assumed to contribute to the shear resistance, but not the area of the concrete arch or fin. The reason for discounting these two resistance components is to ensure a conservative estimate for the FRP capacity, despite the area of the fin being greatest at the location of maximum shear (Hillman 2003). It should be noted that these contributions to shear resistance are focal points within the parallel Virginia Tech investigation.

While the proposed strength design approach is intended to ensure safety, a typical HCB system for highway bridges is controlled by a serviceability criterion, specifically deflection. For the HCB system, the stiffness of the beams varies over the length and thus the moment-area method for calculating deflection is used. The deflections are calculated for the non-composite section with no compressive contribution from the deck, and these deflections are used as the camber built into the formwork for the FRP layup. Due to the deflection-controlled design constraint, additional steel is required to satisfy serviceability limits, making the beam over-reinforced from the ultimate strength perspective. Therefore, unlike traditionally-designed reinforced concrete beams, the failure mode for the HCB will be a sudden and brittle failure of the deck via crushing before the tension steel ever yields (Hillman 2003). However, VDOT anticipates that serviceability limit states for deflection and rideability are likely to be reached prior to the strength limit state.

Benefits, Drawbacks & Unknowns

A topic of interest to some of the preliminary HCB studies (Hillman, 2002) was the feasibility of the system as a viable alternative to existing structural bridge members. There are quite a few features of HCBs that make them attractive to use in both new construction and bridge superstructure replacement projects, but there are also some drawbacks to be considered. Additionally, there are some unknown factors regarding the performance and behavior of the girders that still need to be quantified.

Through use of the concrete arch, a significant quantity of material is saved, which is beneficial both from a constructability and environmental standpoint. The minimization of concrete makes the girders much lighter than ordinary prestressed girders typically required for comparable spans. In some cases there is as much as a 10 to 20% reduction in weight with the deck included (Otter and Doe 2009). Due to the lighter weight of the girders, shipping costs may be reduced since there will be fewer shipments required. Shipping weight may be drastically reduced if the beams are shipped empty and filled with concrete on site. From an environmental standpoint, the production of cement releases large quantities of carbon dioxide into the atmosphere, so any reduction in concrete consumption is better for the environment. Additionally, the lighter shipping weight and fewer shipments require less fuel consumption.

The low weight of the girders may allow for the reuse of existing abutments in many bridge superstructure replacement projects. Large cranes will not be necessary to move the girders into place, and as the girders are self-supporting both under self-weight and the dead weight of uncured concrete, the girders may be placed on the abutments without being filled with arch concrete and eliminate the need for any shoring or deck formwork as the girders themselves serve this purpose (Hillman 2003). Also of importance is the similarity to other bridge construction methods. Once the girders have been fabricated, they resemble a traditional prestressed concrete girder, and require a very low learning curve for installation.

HCBs are also well suited for accelerated bridge construction (ABC) projects as the girders are self-contained, prefabricated units. If the arch concrete is placed within the girder just off-site with adequate curing time, shipping weight will still be conserved, yet the girders can be installed in a minimal amount of time thus minimizing the disruption to traffic flow (Hillman 2008).

Of the few negative aspects associated with HCB use, an important one is the previously highlighted over-reinforced nature of the beams. However, while the high reinforcement ratio can lead to a brittle failure, the additional steel increases the ultimate capacity and provides a significant amount of reserve strength. In some cases, that reserve strength can be as much as four times the design strength (Hillman 2003). The parallel Virginia Tech study is expected to corroborate this characteristic with experimental data. The HCBs tend to be slightly deeper than their prestressed counterparts due to the nature of the arch, which may be of concern to certain users constrained by depth limitations. VDOT provided a rule of thumb for HCB applications which suggests that for the HCB beams should be about the depth of a non-composite steel beam, which is generally shallower than PS bulb tees beams, and deeper than voided slabs or PS box beams in a side by side configuration.

Another drawback is the higher cost of HCBs due to the materials and the labor involved in manufacturing the FRP shell, which have to be laid up by hand and the shell manufacturing process has yet to be automated (Hillman 2003). That being said, should the shell manufacturing process become automated, and as the beams gain traction and are used in an increasing number of projects, the economy of scale should allow for more streamlined manufacturing processes and reduced costs. Still, cost analyses show that the beams are feasible for railway applications in the range of 40 to 60 ft spans, where concrete beams are too heavy for existing rail cranes and steel construction steel is too costly (Otter and Tunna 2011). Additionally, when taking into account the lifecycle cost of the beams, it has been shown that HCBs are cost-competitive in the 30 to 50 ft span range because the higher cost may be distributed over a longer projected service life (Hillman 2003), which is expected to approach 100 years versus the projected 75-year lifespan of concrete girders designed according to the AASHTO LRFD Bridge Design Specifications.

The 100-year lifespan projection has yet to be validated, but has been derived from the FRP shell's ability to protect the internal load carrying components of the beam. The fiberglass is impervious to water and chlorides, thus there is little chance for corrosion of the steel or degrading concrete reactions. In addition, galvanized prestressing steel was used for this particular project to provide additional resistance to corrosion. Furthermore, the FRP weathers well in marine environments, and although is susceptible to degradation from ultraviolet rays, should be adequately protected from sunlight with the concrete bridge deck on top. However, other questions have been raised, including fire resistance and lateral stability in the case of a vehicular collision (Otter and Doe 2009).

Previous Applications and Investigations

IDEAS Program – Preliminary Studies

The first investigation of hybrid composite girders was sponsored by the Transportation Research Board as part of the Innovations Deserving Exploratory Analysis (IDEA) program. The program involved several phases of investigation and was intended to serve first as a feasibility study for HCB application in the bridge market, and second to test prototype beams to determine the reliability of the design philosophy and gather information on the behavior of the complicated beam systems.

The first phase of this IDEA program was a feasibility study that evaluated the cost of producing beams for varying span lengths. Current railway bridge replacement projects became the focus and led to short and medium span bridge applications. The girders were found to be less costly than steel, but more costly than concrete. Hillman (2003) indicated the life cycle costs could still be competitive. In the second phase of the program a single 20 ft prototype beam was constructed in 2003 for testing at the University of Delaware. The girder was 12 in wide by 24 in deep and did not include a composite deck. The beam was simply supported, and loaded in nine different configurations using four actuators distributing load over the span with spreaders. Extensive instrumentation included linear strain gauges throughout the interior of the beam to measure bending stresses and maximum stresses in each material, and deflections were recorded with string potentiometers. The test configurations included

varying loads across the span, mimicking dead loads of a completed rail structure, live loads produced by a Cooper E-80 rail car with impact factors applied, as well as locations of maximum shear and moment. A cyclical load was applied for 100,000 cycles and then the beam was tested for fatigue damage. On the final loading, the beam was tested to failure, sustaining almost 60 kips of load and measuring a deflection just over 2 inches. Although the deflections were greater than predicted, the load tests confirmed the overall design methodology, with the linearly elastic assumptions holding true until just near ultimate loading. An interesting outcome of the study was the discovery that the system acts like a tied arch close to mid-span, but not close to the supports, where the concrete and steel loads diminished as the FRP webs distributed the loads to the supports through shear (Hillman 2003).

A follow-up study supported by the High-Speed Rail IDEAS program was conducted at the Transportation Technology Center, Inc. (TTCI) in Pueblo, Colorado (Hillman 2008). In this investigation, a complete HCB bridge system was used as a replacement bridge for an existing structure operating on the TTCI test track. The bridge, which weighed just 57% of the one it replaced, consisted of 8 HCBs, each 20 in wide by 28 in deep, and bolted side-by-side through their webs into two four-girder groupings. A 4 in composite deck was included, along with ballast curbs and ballast for the rail. The bridge was located on a curved portion of track and thus experienced a slightly inclined loading from the inclined rail and lateral loading from the train as it traversed the curve. Instrumentation for this test included strain gauges and deflection sensors located at strategic positions. The loading program consisted of running heavily loaded freight cars over the bridge, first at static locations to produce maximum shear and moment, then at increasingly rapid dynamic speeds. The testing program demonstrated that the structure behaved in a predictable manner and conformed to the AREMA recommended guidelines. The deformation measurements confirmed that there was indeed full composite action between the deck and girders and all of the strains (stresses) measured were well within the ultimate capacities of each respective material. Limited damage was discovered in the deck concrete, but this shear cracking was due to the eccentricity of the load and not due to any HCB deficiencies. The exterior girders, which supported the ballast curbs always experienced less deflection and strain due to the added stiffness contributed by the curbs.

Advanced Structures and Composites Center – Laboratory Study

A large-scale project was undertaken in 2010 in Boothbay, ME to construct an eight-span HCB bridge spanning a total of 540 ft (Snape and Lindyberg 2009). As part of this project a single beam was tested by the Advanced Structures and Composites Center at the University of Maine. The experimental program included testing for service and fatigue loads both with and without the addition of a composite deck, and finally an ultimate capacity load test. For this project, the girders were 33 in deep with 42 steel strands of 1/2 in diameter, spaced at 4 ft center-to-center such that the FRP wings were integrated with the lid to serve as formwork for the deck in the interstitial space of the beams. Instrumentation included strain gauges internally and externally, LVDTs, string potentiometers, load cells and a 3D digital imaging system to capture surface strains. Instrumentation was primarily concentrated at mid-span, quarter-spans and the supports. The beam was first tested without the presence of a deck, and was subjected

to four-point bending to simulate an HL-93 truck loading. First service shear and moments were determined from static loading, followed by a fatigue loading of 2,000,000 cycles with interim flexural tests to investigate any damage accumulated. The deck was then added to the beam and a similar loading scheme was prescribed. In both cases the beam achieved the predicted strength, although the beam was stiffer than predicted. The higher stiffness was attributed to the contribution of the FRP wings that were neglected in design calculations (Snape and Lindyberg 2009). In addition, there was elastic buckling observed in the FRP lid of the beam during the test prior to addition of the deck, but further buckling was constrained by the deck. The last loading cycle took the beam to ultimate and proved that the beam behaved linearly elastic through failure.

Virginia Tech – Laboratory Study

As part of the parallel study on the HCB system for VDOT, an initial experimental investigation was performed by Ahsan (2012) at Virginia Tech, who was tasked with investigating the HCB system in a laboratory setting, focusing on the element-level behavior and load path generated between the concrete arch and FRP shell, at various phases throughout the construction of the system and a variety of loading scenarios. Of particular interest was a confirmation of the flexural design methodology, which currently uses a transformed sections approach (Van Nossdall et al. 2013). Three HCBs were built for testing according to the specifications used for the proposed construction of the Tides Mill Stream Bridge. An extensive research plan was devised to test the beams throughout the fabrication, and ultimately test a three-girder, fully composite bridge superstructure that would mimic that of the eight-girder bridge design to cross the Tides Mill Stream. The work done on these girders can be separated into three distinct phases. First, the empty FRP box shell (including tension steel) was tested. After placement and curing of the self-consolidating concrete within the arch formwork, a second round of tests were performed to investigate the behavior of the tied arch subjected to construction loads. Lastly, a skewed, three-girder, fully composite bridge superstructure that mimicked the eight-girder design of the Rt. 205 bridge configuration was tested, including a composite deck (Ahsan 2012). Each of these tests was conducted within the elastic range for the structure and components. An extensive instrumentation plan was devised to test the beams at each phase. Strain gauges were mounted externally on the FRP at multiple locations on the webs, top and bottom flanges, and internally on the tension steel. Vibrating wire gauges (VWGs) were also embedded in the arch concrete. Photogrammetry was employed to allow for complex measures of deflection and subsequent derivations of strain on the face of the FRP web. These measurements were confirmed by traditional deflection measurements, including string potentiometers and linear variable differential transformers (LVDTs). Load cells were also used at the bearings to provide a measure of the shear through the beams at the supports.

For testing of the empty FRP box, the lid and wings were placed on top of the shell, but not glued down, all of the dead load could be accounted for, but not add to the flexural rigidity of the box. These beams were tested in a non-skewed configuration, with the same clear span as the Rt. 205 Bridge. The loading consisted of steel angles

spaced closely along the length of the beam. Ahsan found that the FRP behaved in a linear elastic manner under this loading configuration.

The next phase tested a series of completed HCBs, which included the arch concrete and the FRP lids glued to the top of the beams. These beams were also tested in a straight configuration with the same clear span. The two loading scenarios for these beams involved a single load point of 15 kips at mid-span, and two third-point loads of 12.5 kips. As anticipated, the FRP did not contribute significantly to the flexural strength of the overall beam, with the tied concrete arch carrying approximately 80% of the total flexural load, leaving the shell to carry the remaining 20%. In comparing the strain registered on the steel itself and the FRP surrounding the steel, there is relatively good strain compatibility in the tension zone (Van Nosedall et al. 2013).

The final experiments consisted of tests of a three-girder mockup of the fully composite HCB system as would be put in-service at Colonial Beach. It is important to note, however, that the bridge mockup did not include any parapet walls nor was there any mechanism to enforce the fixity caused by the integral abutment backwalls that were part of the actual bridge design. The AASHTO HL-93 design truck was used as the loading configuration with an additional 33% increase to account for dynamic amplification effects. Several simulated wheel path configurations were tested to induce a variety of moment and shear distributions throughout the system. Once the beams became composite with the deck, the neutral axis moved up within the deck. Thus, the HCB ceased to act as a tied arch, and the concrete arch contributed little to the strength of the system. The researchers was also found that the FRP shell and tension steel combined to provide 80% of the total flexural resistance, while the deck accounted for the remaining 20% (Van Nosedall et al. 2013). A number of additional findings were also reported by (Ahsan 2012) that have direct relevance to the field testing in this current study including:

1. It was determined that the concrete arch does not act compositely with the rest of the HCB system. Ahsan (2012) hypothesized the existence of a local bending phenomenon of this thin arch that is accentuated at the unsupported quarter-spans. The tension strains registered in the bottom of the arch are not compatible, but quite exaggerated compared to the strains read from the external FRP strain gauges, indicating the existence of this phenomenon. Further, there exists a discrepancy between the upper and lower strain readings in the arch also indicating flexure within the arch. Figure 2 shows an adaptation of the phenomena described by Ahsan. In this theory, the mid-span of the arch is treated as being supported by a stiff spring, as an 8 ft FRP sheet connects the two FRP webs directly beneath the arch conduit. From a practical perspective, the purpose of this sheet was to provide a rigid surface to protect the foam formwork from the force of the concrete placed at this location, and preserve the shape of the arch. Following this theory, it is easy to see how flexure could be induced throughout the length of the arch, but especially at the unsupported quarter points.

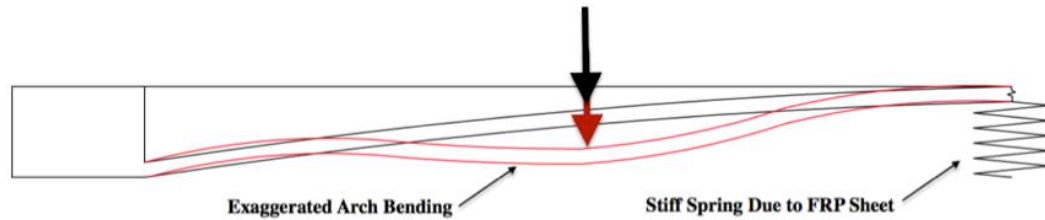


Figure 2 - Thin Arch Local Bending Hypothesis (Adapted from Ahsan 2012)

2. The tensile strains registered in the bottom of the arch were found to be well above that necessary to induce cracking in this concrete, yet there clearly was a means to carry this level of strain during the test. The strain readings indicate that the two steel strands laid out in the bottom of the arch profile for construction purposes may also provide tensile resistance within the arch (Ahsan 2012).
3. Ahsan (2012) included an analysis of both moment and shear distribution factors from the limited load configurations performed on the three-girder system and provided a comparison to the assumed AASHTO values. While the design for this bridge was conservative and does not include skew corrections, Ahsan included lever rule corrections in his calculations and found the exterior girder shear and moment distribution factors to be within AASHTO regulations. Interior distribution factors were less conservative as compared to the AASHTO values.

Experimental Program

Tides Mill Stream – Route 205 Bridge Fabrication and Construction

The live load testing program focused on the newly constructed HCB bridge on Route 205 over the Tides Mill Stream in Colonial Beach, VA (Figure 3). Beam fabrication took place in a series of stages (Figure 4), so the internal instrumentation followed this construction sequence. The HCBs shells and lids were fabricated off site, at Harbor Technologies in Brunswick, ME. During this fabrication phase the box shells were laid up with fiberglass, high-strength passive steel strand and foam were placed in the formwork and then infused with resin. In this manner, eight lightweight, self-supporting, monolithic box shells were created and shipped to Coastal Precast concrete plant in Virginia, where they were filled with self-consolidating concrete and allowed to cure, forming a fully functional, composite HCB girder. These girders were placed on the existing abutments that were being reused and the ends were encased in integral backwalls, resulting in semi-integral abutments. From that point, the steel reinforcement mat for the deck was constructed, and construction began to take the form of a conventional bridge project.

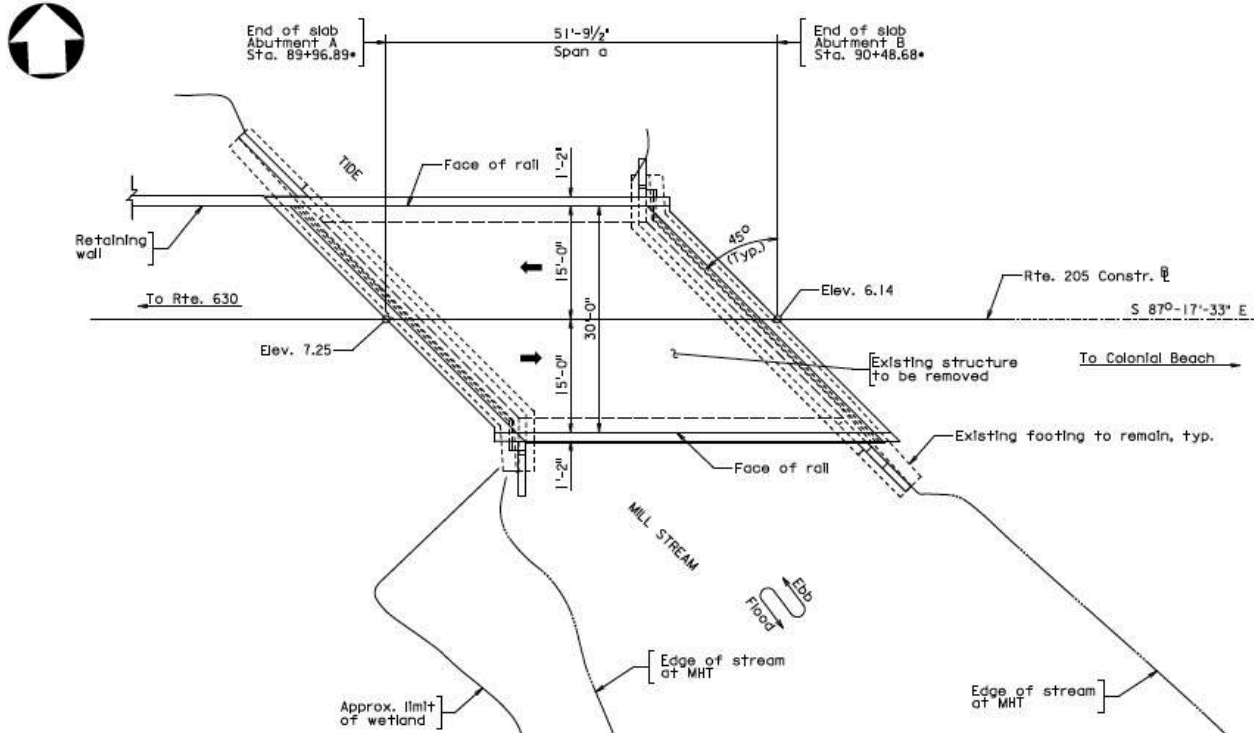


Figure 3 – Tides Mill Stream Site – Plan View



(a)



(b)



(c)



(d)

Figure 4 – HCB Fabrication Process (a) glass fiber fabric, (b) foam inserts, (c) completed HCB box, and (d) placement of SCC within HCB arch

The previous concrete girders and deck were replaced with eight HCBs spanning 44 ft over a small creek and supporting a 7.5 in deep conventionally reinforced, cast-in-place concrete deck, while maintaining the existing substructure. Each HCB girder was 21 in deep by 24 in wide and contained inclined shear connectors that enforced composite action between the HCB and the concrete deck. The girders were spaced at ~ 4 ft center-to-center, yielding a 32'-4" transverse width that allowed for two lanes of traffic with 3 ft shoulders (Figure 5). The girders were skewed at 45° and supported by two parallel abutments, and the ends were encased in integral abutment backwalls, resulting in semi-integral abutments. The girders crossed the waterway with a very low clearance of approximately 6 ft at low tide, making access for instrumentation a challenge. The stream feeds to the Potomac River, which flows to the North of the bridge site.

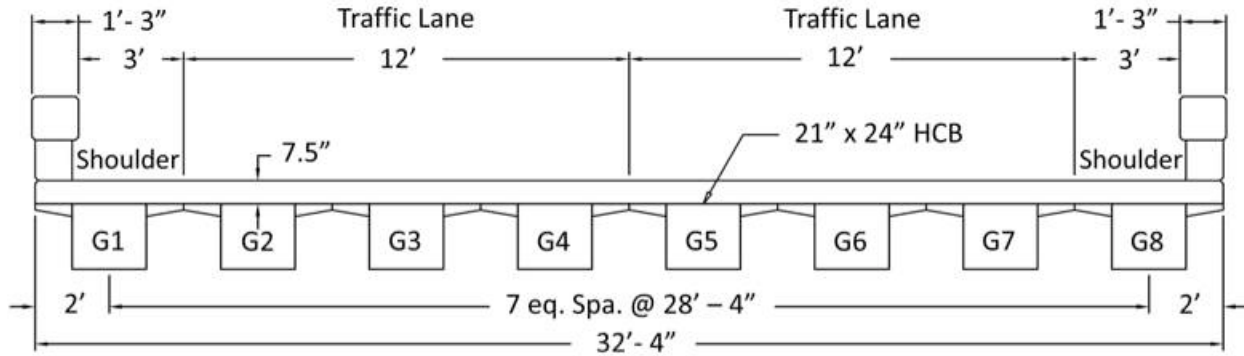


Figure 5 – Tides Mill Stream – HCB Bridge Cross-Section

Instrumentation & Experimental Setup

To satisfy the testing program and establish a mechanism for monitoring, an extensive instrumentation plan was developed. The program required a variety of sensors with multiple data acquisition systems. To keep the instrumentation systems organized, a nomenclature for the girders was established (Figure 6) where the northernmost girder was labeled number 1, and the numbers progressed sequentially to the eighth and southernmost girder, labeled girder 8. The various acquisition systems and their functionality are described in further detail in this section. The first data acquisition system used a series of Campbell Scientific Inc. (CSI) dataloggers that monitored internally mounted vibrating wire gauges (VWGs) that were installed throughout the fabrication and construction phases of the girders and bridge deck. The second data acquisition system was deployed on the day of testing only and used a rapidly deployable wireless field-testing setup by Bridge Diagnostics Inc. (BDI) which primarily used externally mounted strain gauges. It should be noted that both the internal and external gauges were intended to be used during load-testing, but only internal VWGs were intended for long-term monitoring due to their durability and the protection offered by embedment.

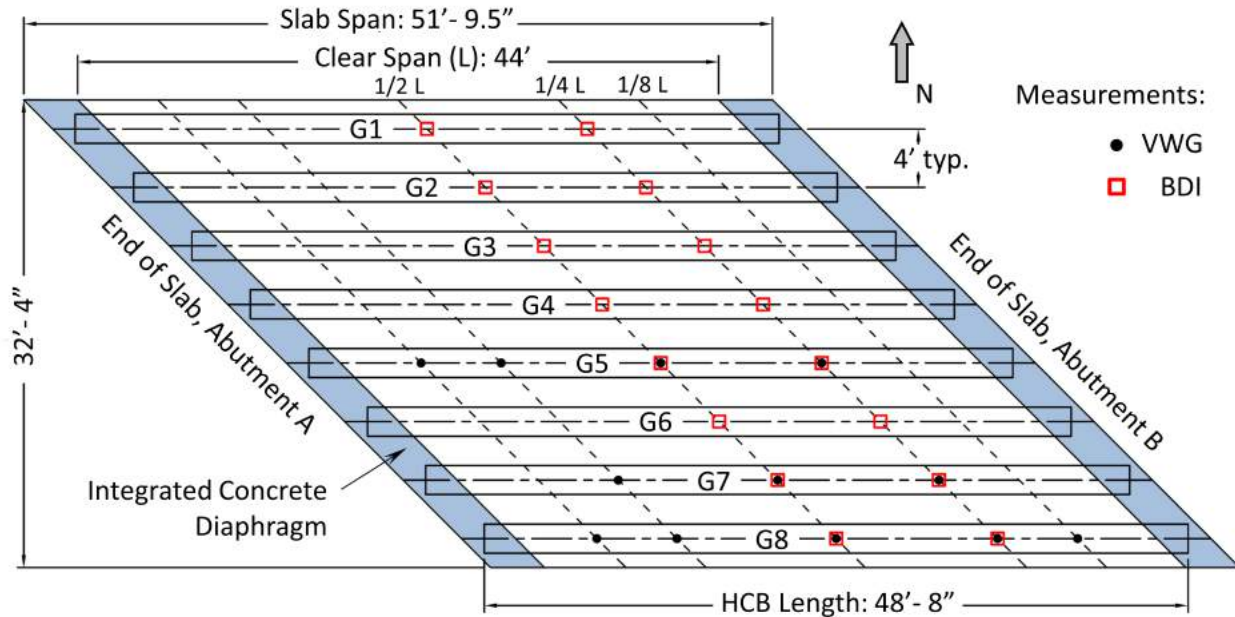


Figure 6 – Bridge Nomenclature with Instrumentation Overview (plan view)

Campbell Scientific Data Acquisition and Gauge Installation

The CSI system provided the capability to measure internal system response during both short-term live load testing and long-term monitoring. Geokon 4200 series embeddable VWGs were used and two separate Campbell Scientific Inc. (CSI) data acquisition systems (DAQ) were selected for measurement. The first CSI DAQ (CR 1000/ AWV200/AM32B) was intended for long-term periodic monitoring and provided static-only measurements of select VWGs. This system was limited to a total of 48 VWGs. Similarly, the second CSI DAQ (CR 3000/SC-CPI/CDM-VW305) provided the ability to interrogate VWGs statically, but also provided the capability of interrogating the VWGs dynamically. This dynamic capability was a new capability available from CSI and this investigation provide a preliminary trial of the system. While these systems proved functional, the acquisition of data during the live load testing program was unsuccessful due to programming errors resulting in the data being overwritten. Nonetheless, this information is included herein because the sensors are available for long-term monitoring and future load testing.

The locations of vibrating wire gauges were selected to capture enough of the desired behavior, while remaining reasonably economical. A total of 48 VWG locations were selected and these VWGs were installed in three of the eight girders (girders 5, 7, and 8) so as to minimize the interference with the construction of the girders. Symmetry of the bridge made this instrumentation plan feasible, as it was still possible to capture both acute and obtuse corners of the skew. Figure 7 and Table 1 illustrate and describe the location of the gauges within the HCB cross-section, while Figure 6 illustrates the selected longitudinal and transverse locations.

Along the length of the three selected beams, gauges were installed at mid-span to yield the maximum flexural responses of these select girders, and at both the quarter-span locations to capture the effect of the skew. Additional gauges were installed at

select eighth-span points in a 60° rosette configuration on these three girders to measure shear response.

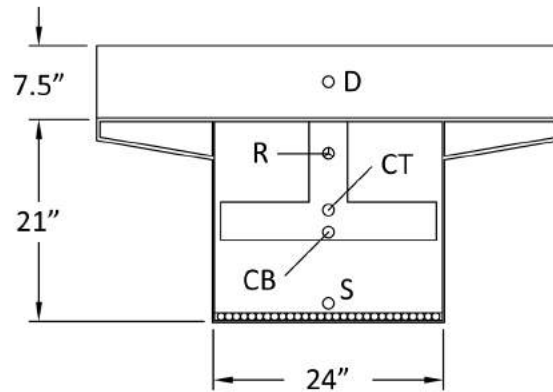


Figure 7 – General Vibrating Wire Gauge Locations through the Depth

Table 1 - Vibrating Wire Gauge Instrumentation Location Matrix

	Girder 5	Girder 7	Girder 8
East Eighthspan			<i>R, CT, CB</i>
East Quarter-span	<i>D, CT, CB, S</i>	<i>D, CT, CB, S</i>	<i>D, CT, CB, S</i>
Mid-span	<i>D, CT, CB, S</i>	<i>D, CT, CB, S</i>	<i>D, CT, CB, S</i>
West Quarter-span	<i>D, CT, CB, S</i>	<i>D, CT, CB, S</i>	<i>D, CT, CB, S</i>
West Eighthspan	<i>R, CT, CB</i>		<i>R, CT, CB</i>

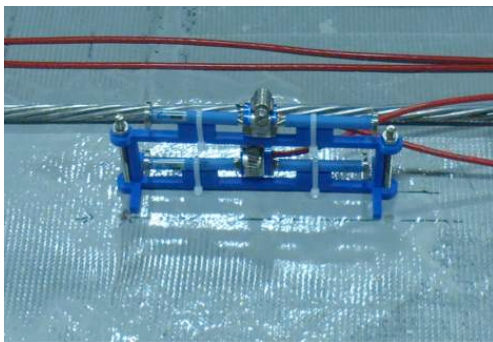
D = deck; *CT* = upper arch; *CB* = lower arch; *S* = tension strand; *R* = rosette within the fin

During the first phase of fabrication of the HCBs, the fabrication of the FRP box shell, a VWG was installed at each of the nine proposed mid-span and quarter-span locations at the level of the steel strand. This involved tying the VWG parallel to a tension steel strand as close to the middle of the girder as possible during the layup of the fiberglass sheets and high-strength steel strand (Figure 8). Just as concrete transfers strain to a VWG through the movement of concrete perpendicular to the end discs, it was theorized that when cured, the resin would offer the same transfer of strain to the gauge and an accurate reading would be provided for the particular cross-sectional depth.

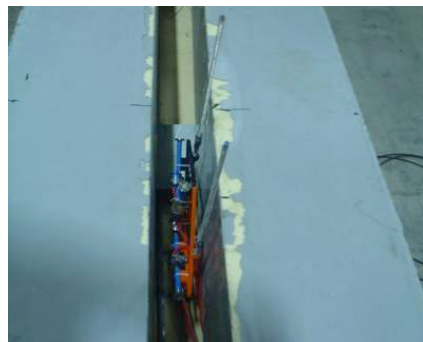


Figure 8 - Internal VWG Placement at Tension Level

After infusion of the FRP shell, the remainder of the VWGs internal to the HCB itself were installed. A series of non-corroding, acrylonitrile butadiene styrene, 3D-printed frames were designed to hold the VWGs in place at the desired location within the voided conduits that would later be filled with SCC. Again, nine frames were placed at the proposed mid-span and quarter-span locations with two VWGs stacked two inches apart. Each frame was then inserted through the void for the concrete fin (Figure 9a) down to the level of the arch void and inserted into the existing foam formwork such that the VWGs were aligned longitudinally and horizontally with the beam, not parallel to the slope of the arch. Note that the exact cross-sectional depth of these gauges differed by location due to the varying profile of the parabolic arch. At the three designated eighth point locations, a frame identical to the one devised for the other arch locations was used in conjunction with an additional frame on top of the first. This added frame held three VWGs arranged in a 60° rosette. The rosette was designed to measure the shear in the fin near the point of maximum shear and where the fin is deepest.. The two frames were linked by two stainless steel threaded rods that enabled the whole assembly to be lowered into the deeper eighth-span locations (Figure 9b).



(a)



(b)

Figure 9 – Stacked Strain Gauge Configuration (a) Concrete Arch VWG Frame at Mid-span and (b) Additional Rosette Configuration at Eighth-span

After placement of the internal concrete within the HCB, the beams were positioned on site, and the deck reinforcement mat was laid out. Nine additional gauges were longitudinally affixed to the mat 4 in deep at companion locations to the mid-span and quarter-span locations of the three selected girders prior to placement of the deck concrete (Figure 10). The resulting system of gauges was expected to provide a more comprehensive measure of the overall internal system behavior including the neutral axis location and level of composite action between the deck and girders. However, despite the successful implementation of the internal VWG's, data for only 15 sensors were recorded during the test due to limitations associated with the CSI acquisition system, which was limited to 16 input channels. In addition, no data was collected from the Rosette-configured strain gauges.

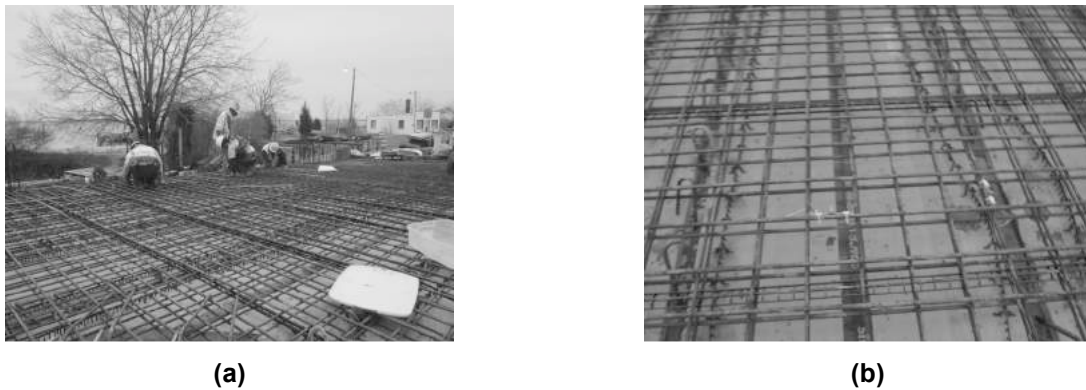


Figure 10 – Instrumentation for Concrete Bridge Deck (a) gauge layout and (b) installed VWG

Bridge Diagnostics Data Acquisition System and Gauge Installation

The second data acquisition system was deployed on the day of testing only and used a rapidly deployable wireless field-testing setup by Bridge Diagnostics Inc. (BDI), which primarily used externally mounted strain gauges. The external BDI strain gauges were placed in conjunction with the internal VWGs in order to mirror the strain locations and provide a comparison between the internal strains and the strains experienced by the external FRP shell (Figure 6 and Figure 11). These external gauges were mounted on the bottom flange of each girder at mid-span and the East quarter-span to capture distribution behavior laterally across the eight girders. Additional gauges were mounted on the web of the girders at these locations as close to the arch position as possible, though the depth of the wings made this somewhat challenging at mid-span. These web gauges were used to create an external strain profile that could be aligned with the internal strain profiles and contribute to the evaluation of the load sharing behavior of the individual HCB elements. Lastly, two additional external BDI strain gauges were placed on the parapet at mid-span such that any strains registered could give an indication of the level of stiffening provided by the barriers to the bridge system. A BDI string potentiometer was also used to measure deflection for the northern exterior girder; however, the anchorage system for the string pot was insufficient to maintain the required tension and was therefore not included in this report.

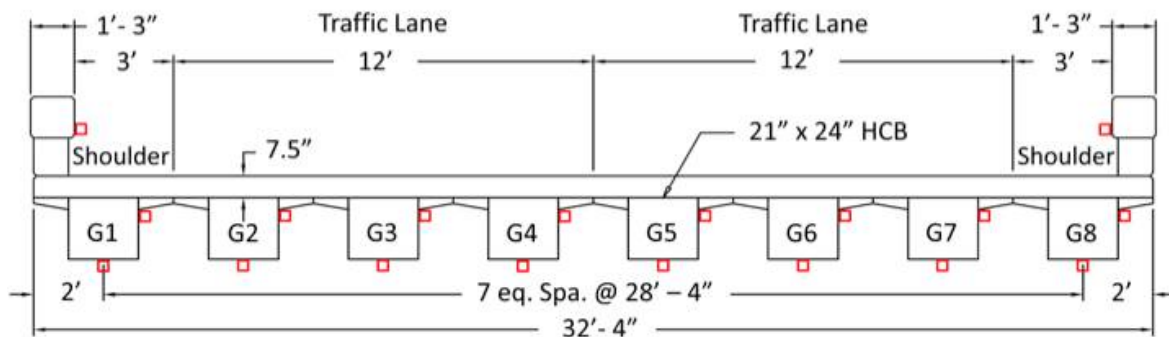


Figure 11 – Tides Mill Stream Bridge Cross-Section with Midspan External Strain Gauge Configuration

Experimental Set-up

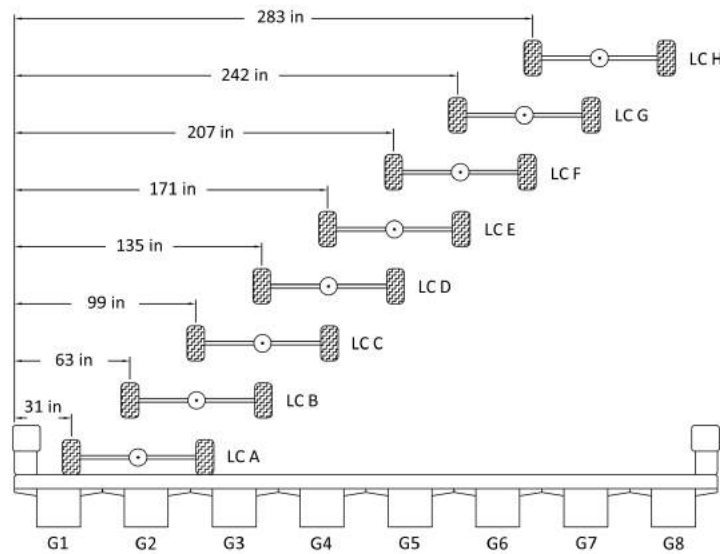
The instrumentation was performed over two days between August 5th-6th, 2013. The first day consisted mostly of setup and preparatory work and the second day included final preparation and carrying out the load test runs. It was a function of the bridge site that the clearance of the waterway was already shallow, but the clearance between the bridge and stream also fluctuated with the rising tides. This was a concern that had to be factored into the schedule of the load test, and dictated when certain tasks could be performed underneath. This factor determined the need to carry out the load test over two days. The depth of the waterway varied, and as such, a combination of small jon boats and researchers in waders was used for access to attach the sensors beneath the bridge.

On the morning of August 5, two teams worked to accomplish multiple tasks. One team was responsible for affixing the BDI strain gauges to the underside of the bridge using a very rapid-set epoxy. The bottom flange gauges were aligned and centered on the flange, while the additional longitudinal gauges were adhered 1.5 in. beneath the wing edge on the south-facing web. The underside installation and began marking mid and quarter-span locations with measurements taken from the clear span distance, and a chalk line was dropped across all eight girders, along the skew to mark these locations on each beam. To keep the sensor lead wires organized and dry, conduit clamps were glued along the girders and the lead wires were sequentially zip-tied to the clamps, channeling the groupings out the South end of the bridge where they were bundled and bagged to keep moisture out overnight. These bundles were then hung on conduit clamps on the first interior web, or rested on the abutment face to remain out of sight.

The second team was responsible for marking the pre-determined wheel paths or load cases (Figure 12) and organizing the BDI wireless nodes as input channels. It was important to place specifically labeled gauges at the predetermined locations for data analysis, however the BDI system does not require one to plug in the gauges in any particular order.



(a)



(b)

Figure 12 – Wheel path (a) Markings and (b) Configuration

On the morning of the load test, the BDI wire leads were retrieved from under the bridge and connected to the wireless BDI nodes, which were in turn connected to the wireless base station, which communicated wirelessly with the computer controlling the system. Also, pre-made cardboard shields were mounted to protect the externally mounted strain gauges from wind, as other researchers have noted that BDI strain gauges tended to have a sensitivity to wind currents. Along with the BDI system, the lead wires from the internally mounted VWGs were connected to the appropriate CSI datalogger for periodic measurements. For live load testing it was necessary to disconnect 15 pre-select gauges to be measured dynamically and set up the dynamic CSI system (CR3000). For the VWGs remaining on the “static” datalogger system (CR1000), the measurement and recording frequency was limited due to the speed of the datalogger and required about a minute to cycle through all of the gauges sequentially. Therefore, the load truck was parted at predetermined locations during the third run of each test to allow the “static” datalogger sufficient time to acquire the measurements. In addition to the instrumentation on the bridge, a BDI product called an

Autoclicker was attached to the wheel well of the load test truck to track the time and longitudinal position of the truck as it crossed the bridge.

Load Testing

The load test was performed on the afternoon of August 6 by driving the load vehicle East to West across the bridge at predetermined transverse positions as shown in Figure 12. The load trucks that were used were VDOT tandem-axle dump trucks loaded with gravel (Table 2). Truck RO6187 was used for the static test configurations while Truck RO9185 was used for the dynamic tests. The change in truck between the two sets of tests was necessary due to a damaged grease socket on the driver’s side front wheel that occurred at the end of the static testing program.

Table 2: Load Test Truck Specifications

	Truck RO6187 (Quasi-Static)	Truck RO9185 (Dynamic)
Front Axle Weight	18.12 kip	17.32 kip
Rear Axle Weight	33.98 kip	33.20 kip
Total Truck Weight	52.10 kip	50.52 kip
Front Axle Width (center-to-center of tires)	82 in	79 in
Rear Axle Width (center-to-center of tires)	73 in	73 in
Tire Width	10 in	10 in
Front Axle Span	165 in	162 in
Rear Axle Span	53 in	55 in
Single Tire Rotation Travel Distance	129 in	--

Static Testing

During static testing, the truck was positioned in each of the eight different transverse locations in order to elicit a maximum response from each of the eight girders. In each scenario, the truck driver was guided (Figure 13) to ensure that passenger’s side wheel path aligned with the designated paths marked on the bridge deck and proceeded along the bridge at an idle speed that was less than 5 mph. Thus, much of the static testing was more quasi-static in nature. That data for the static testing was captured at 25 Hz for the BDI system and 100 Hz for the CSI dynamic system; the CSI dynamic system also recorded a separate dataset at 1 Hz. Each transverse run was performed a total of three times, where the third run was paused for 60 seconds close to the midspan of the girder nearest the driver’s side wheel path. This pause was intended to allow the remaining non-dynamically monitored VWGs to collect a true static picture of the loaded configuration. These static tests provided critical information regarding the system-level load sharing behavior as well as internal composite load sharing behavior of the HCB system.



Figure 13 – Static Load Testing with Truck Guided Along Wheel Path A

Dynamic Testing

Truck RO9185 was used for the dynamic testing. A series of baseline static test runs were performed with this truck to provide a reference for the dynamic measurement. The load configurations for the baseline and dynamic testing were limited to positions 'B' and 'D'(Figure 12); these positions were selected because of the ease of traveling at the posted speed limit and maintaining the proper travel path. Traversing the bridge in the eastbound lane at the posted speed limit was not possible due to the curvature of the approach roadway. For ease of navigation, the wheel path lines marked on the bridge were adjusted to allow for the driver to follow the path along the driver's line of sight rather than the passenger's wheel line. At each of the two locations, 2-3 dynamic runs were performed near the posted speed limit (between 35-45 mph). During the dynamic load testing, the data was captured at 200 Hz for the BDI system and 100 Hz for the CSI dynamic system.

Results and Discussion

Following the completion of the load-testing program, the data were retrieved from the data acquisition systems and post-processed by the research team. Upon retrieval of the data, it became apparent that a number of holes existed in the collected datasets, primarily within data collected using the the long-term monitoring system CSI DAQ (CR 1000/ AWW200/AM32B). Unfortunately, this system was not successfully deployed during the load testing and, as a result, none of the data from the secondary sensors were collected during the parked loading scenarios for each load configuration. In addition, the dynamic CSI DAQ (CR 3000/SC-CPI/CDM-VW305) had limited memory and ended up overwriting data collected during the load testing. However, while the dynamic data was not collected with this system, the internal gauges connected to the dynamic system were interrogated at a frequency of 1 Hz, which allowed for part of the static data to be salvaged. Processing the available data, the following behavior characteristics were evaluated:

- Lateral Load Distribution – a phenomena that describes the transverse load sharing behavior of a beam bridge system and a fractional measure of how much load is resisted by an individual member. The fractional representation

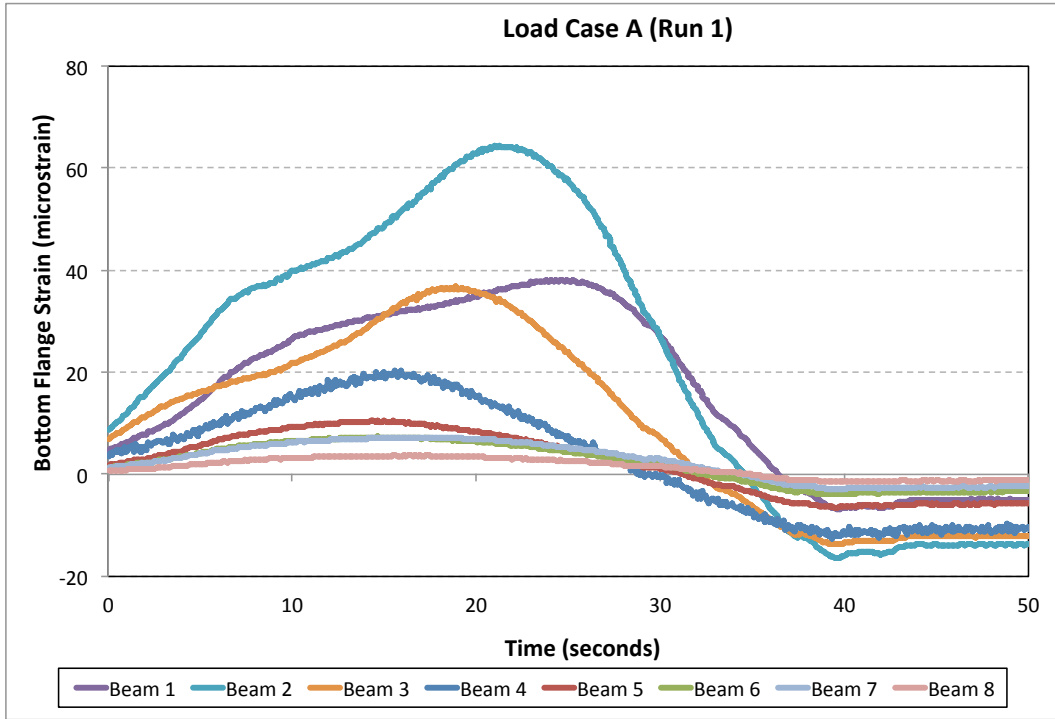
is generally considered a simplification of complex two-way bridge system interactions down to a one-way behavior representation and is typically used for member design.

- Internal/External Load Sharing Behavior – the relative load sharing behavior for the HCB system that describes the relative contribution of the internal (concrete arch and prestressing steel) and external (FRP shell) components.
- Dynamic Load Allowance – the amplification of load above that of the static loading that occurs during dynamic loading. This phenomena is typically described as a function of the interaction of the bridge and vehicle dynamic response interaction and is influenced by properties such as mass, stiffness, vehicle speed, and surface roughness.

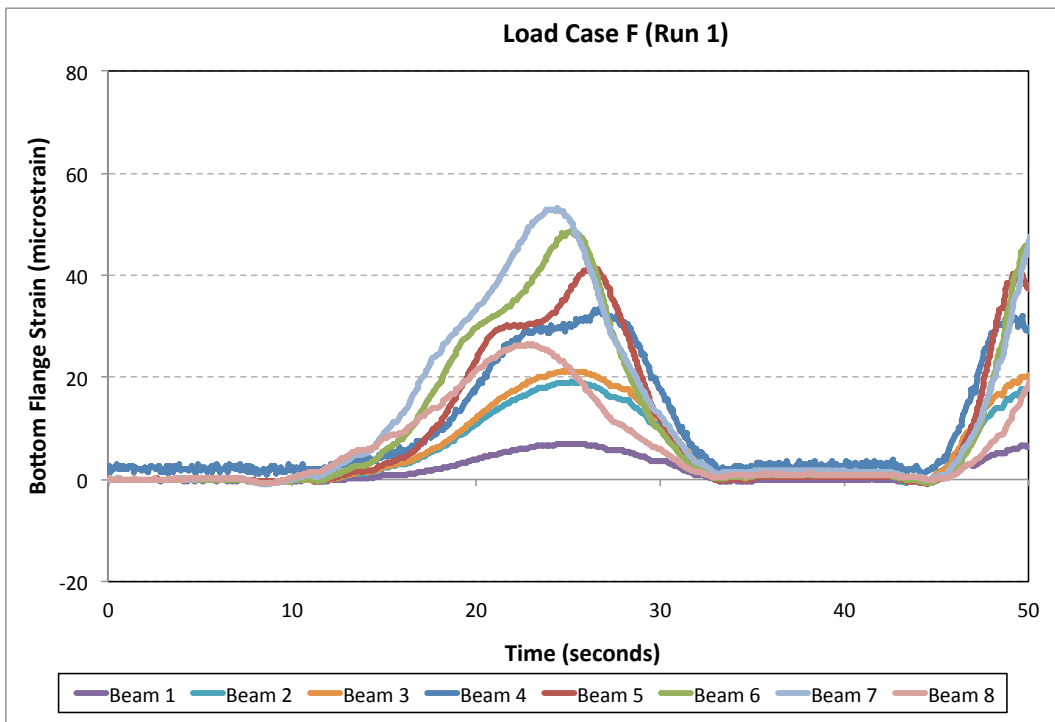
Flexural Lateral Load Distribution Behavior

In this study, the flexural lateral load distribution behavior was analyzed to help evaluate the in-service behavior of the HCB bridge because such in-situ performance is critical to the end user, yet there is very little data available in this regard. Within a typical beam bridge structure, the expected behavior under load is that the girders most directly under the loading will resist the majority of the load, with the girders further away resisting less. This phenomena is illustrated in Figure 14 which presents the select time series strain data for Load Case A (Run 1) and Load Case F (Run 1). For the Load Case A, Beam 2, which is straddled by the load truck, clearly experiences the greatest amount of strain with lower magnitudes of strain observed in the two adjacent beams (Beams 1 and 3). It is interesting to note that Girder 1 would be expected to also have sizable response, but this effect is somewhat muted by the influence of the parapet. A similar response is observed for Load Case F, where Beam 7 exhibited the largest strain response relative to the adjacent beams.

The lateral load distribution behavior is influenced by a number of factors including girder spacing, deck thickness, span length, and girder stiffness. As previously highlighted, the most heavily loaded girders experience the greatest bottom flange strain and internal strain, while girders further away experience less (see Figures 15-22). For the loading scenarios where the truck is positioned near the exterior of the bridge (e.g. Load Case A and Load Case H), an interesting phenomena is observed in the strain profiles which suggests that there is a significant contribution provided by the parapet wall, which carry a fraction of the load, as evidenced by the decrease in strain in the exterior beams. In the Virginia Tech study, Ahsan (2012) observed a similar distribution response for the interior girder, but the exterior stiffening effects were not present due to the lack of parapets in those tests. It should also be noted that this phenomena was not observed in the internal VWGs, likely due to the non-composite behavior between the internal and external beam components.



(a)



(b)

Figure 14 – Time Series Strain Data (All Beams) – Static Loading (a) Load Case A1 and (b) Load Case F1

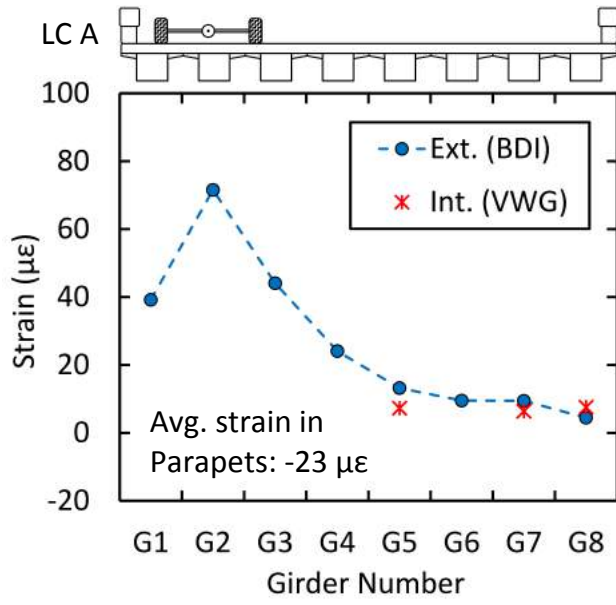


Figure 15 – Tensile Zone Strain (LC A)

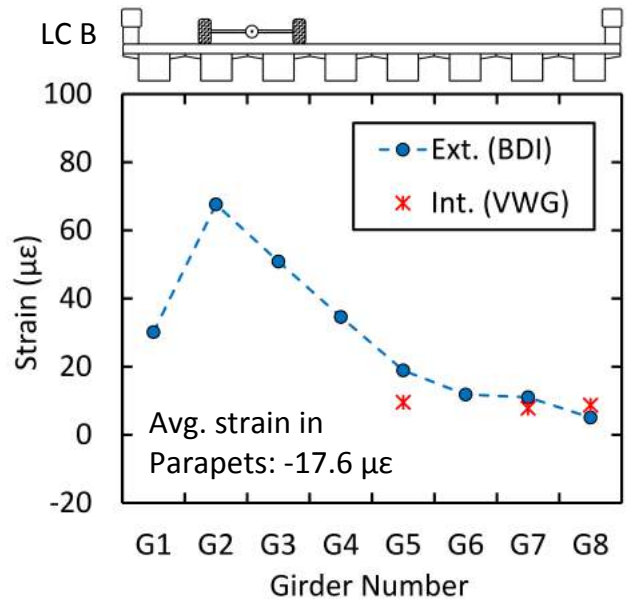


Figure 16 - Tensile Zone Strain (LC B)

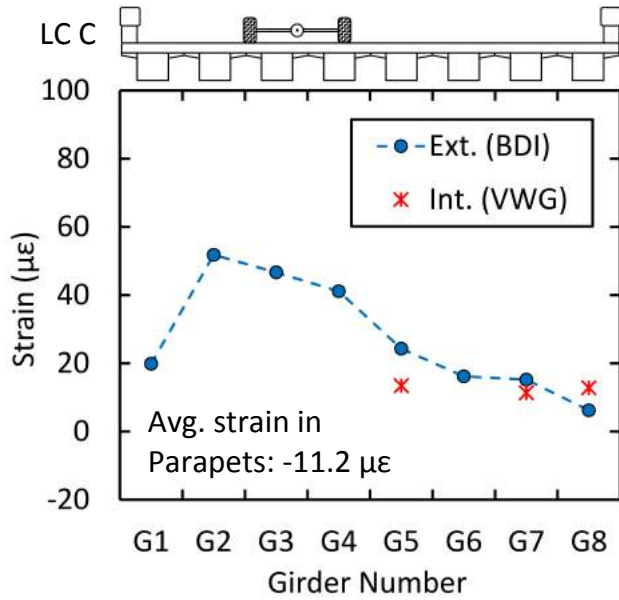


Figure 17 - Tensile Zone Strain (LC C)

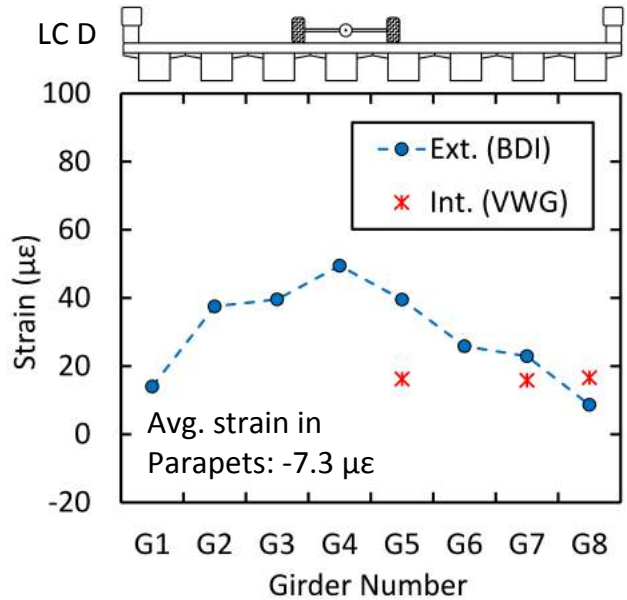


Figure 18 - Tensile Zone Strain (LC D)

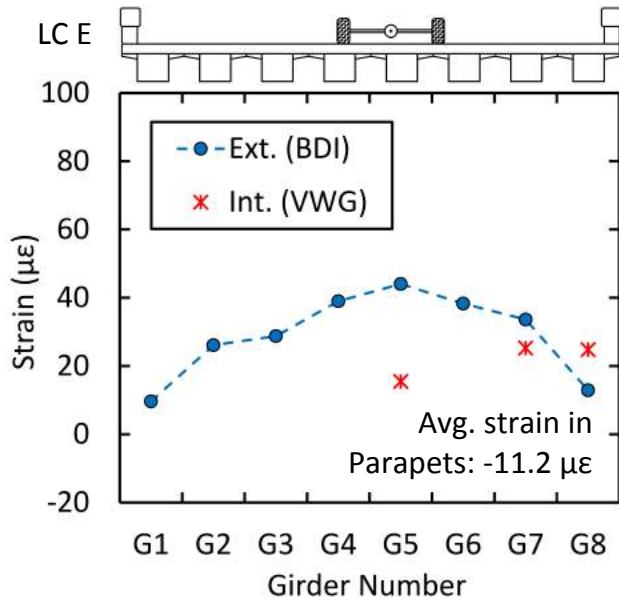


Figure 19 - Tensile Zone Strain (LC E)

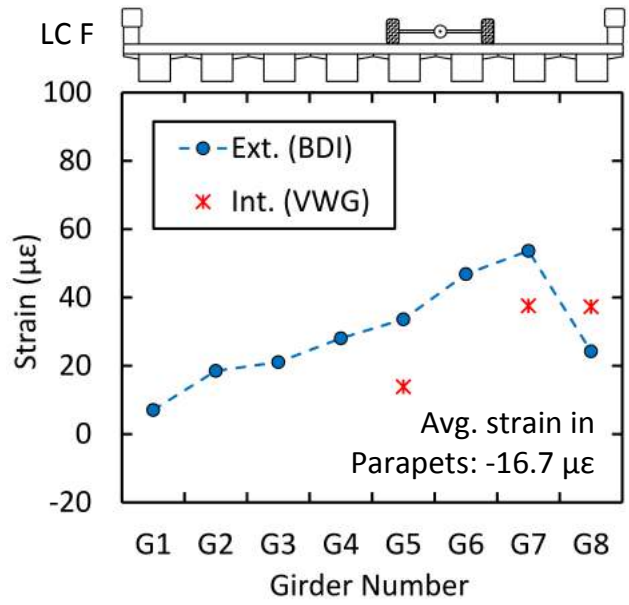


Figure 20 - Tensile Zone Strain (LC F)

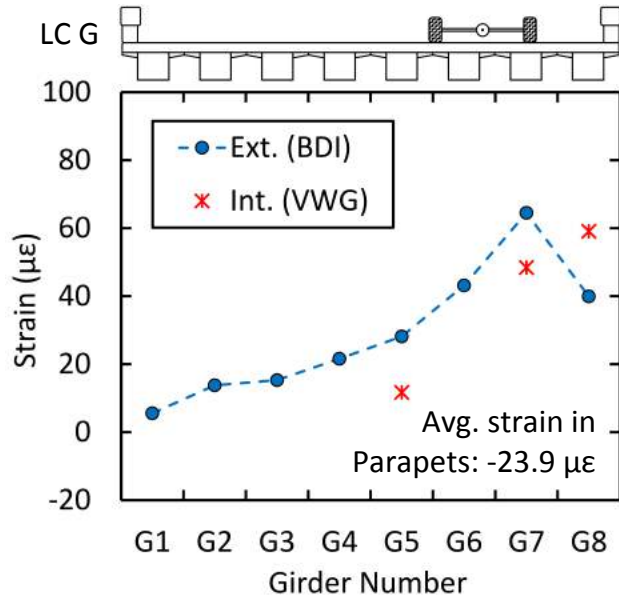


Figure 21 - Tensile Zone Strain (LC G)

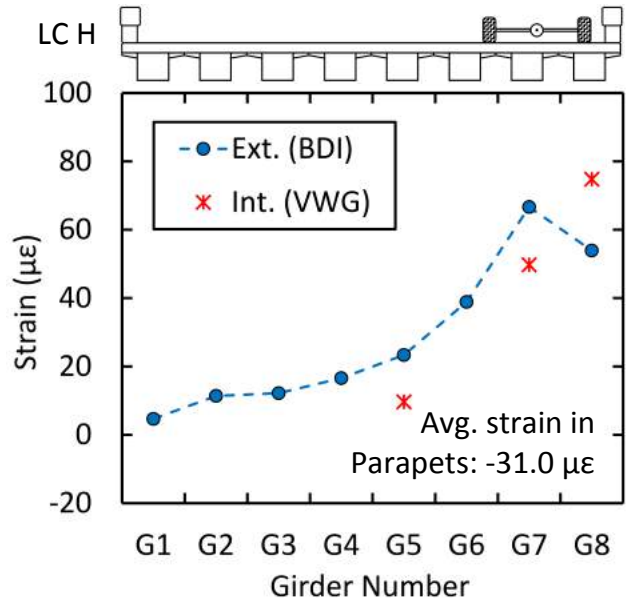


Figure 22 - Tensile Zone Strain (LC H)

When comparing the strains observed on the exterior (BDI) with those measured internally (VWG), the VWG strains do not consistently match the same trend for lateral load distribution. The internal strain readings are consistently lower than the external FRP strains, with the exception of the fascia girder number 8. The cause of this non-correspondence is unknown, but may be attributed to the non-composite behavior of the HCB components, as discussed in the next section on element load sharing behavior. This non-composite behavior theory is also reinforced by an observation of the strains

near the exterior of the bridge near the parapet walls where there is a lower stiffening effect on the internal tension strands than the FRP shell.

The lateral load distribution response, as previously defined, describes the relative load fraction resisted by each girder within the system. Equation 1, is commonly used to describe the flexural lateral load distribution response (Eom and Nowak 2001; Waldron et al. 2005; Harris et al. 2008; Harris 2010), where strains at mid-span are the measured inputs. Using this relationship, the average maximum distribution factors for each of the load configurations are summarized in Table 3. The values presented in the table include the controlling or maximum distribution factors for both the interior and exterior girder locations as described by AASHTO (2012) and are aligned with the measured response of the most heavily loaded beam for each load case. Also included are the calculated flexural distribution factors from the AASHTO LRFD Bridge Design Specifications (2012) for the cases of conventional slab-girder bridge system such as a concrete deck on reinforced concrete girders (AASHTO Type A) or a concrete deck on box girders (AASHTO Type B), as well as the calculated values from the historical AASHTO Standard Specification (2002). Results from the three-girder HCB system tested at Virginia Tech (Ahsan 2012) are also included for reference.

For the load-testing program, the controlling distribution factor for the interior girder resulted from Load Case A, while the controlling value for the exterior girder occurred for Load Case H. This exterior girder response highlighted the effect of the skewed configuration on the lateral load distribution behavior of the system. Despite the almost symmetric loading conditions (A compared to H) and symmetric cross section of the bridge, the skew caused the exterior girder to behave differently on opposite sides of the bridge, with lower exterior distribution factors measured for Load Case A. The interior distribution factors from the field test were slightly lower than the results from the study by Ahsan (2012), indicating a more uniform load sharing phenomenon than was found in the full-scale laboratory testing. This is not surprising considering the Tides Mill Stream Bridge had more beams to distribute the load amongst. Furthermore, the measured exterior distribution factors were lower than the laboratory values, most likely due to the absence of the parapet walls in the preliminary study.

When comparing the field test results to the AASHTO provisions, it should be emphasized that the AASHTO LRFD and the AASHTO Standard Specifications do not contain provisions for the HCB system. Nonetheless, the anticipated HCB element behavior was something similar to that of a conventional slab-girder bridge system such as an concrete deck on reinforced concrete girders (AASHTO Type A) or a concrete deck on box girders (AASHTO Type B). Even when accounting for code-specified adjustments for skew, the Type A and Type B designations yielded conservative estimates for the exterior girders compared to the experimental results. On the other hand, only the Type A design value was conservative for the interior distribution factor.

$$DF_i = \frac{\epsilon_{\max i}}{\sum_{i=1}^{\# \text{ girders}} \epsilon_{\max i}} \cdot (\# \text{ of Trucks})$$

Equation 1

Table 3: Summary of Mid-span Flexural Distribution Factors

	Max. Exterior	Max. Interior
Load Test Results		
Load Case A	0.188	0.349
Load Case B	0.135	0.316
Load Case C	0.094	0.256
Load Case D	0.059	0.220
Load Case E	0.051	0.199
Load Case F	0.103	0.230
Load Case G	0.164	0.281
Load Case H	0.225	0.298
Controlling	0.225	0.349
AASHTO LRFD		
Cast-in-place concrete deck on steel or concrete beams (Case A)	0.247	0.360
Cast-in-place concrete deck on closed steel or precast boxes (Case B)	0.288	0.306
AASHTO Standard Specification		
	0.371	0.371
Virginia Tech (Ahsan 2012)		
	0.390	0.360

Element Load Sharing Behavior

The HCB system is a composite system that is constructed in multiple stages and as a result, characterization of the internal element level load sharing behavior is critical. An understanding of this internal load sharing behavior is also essential for maintenance and decision-making processes as the system ages. The internal (VWG) and external (BDI) instrumentation allowed for the measurement of the strain profile through the depth of girders 5, 7, and 8 during loading. The data provided critical information on the load sharing behavior between the concrete arch, FRP shell, and reinforcing steel, as well as the location of the neutral axis of the composite cross-section. One critical note is that while the HCB is designed as a tied arch system, once the deck is cast, the neutral axis occurs in the deck. Thus, the entire HCB, including the arch, can be expected to be in tension, including the arch, at mid-span under superimposed dead load (Van Nossdall et al. 2013).

Figure 23 - Figure 26 illustrate the midspan strain profiles through the depth of the cross-section for beams 5, 7, and 8 subjected to Load Cases A, F, G, and H. Load Case A is presented merely for illustrative purposes, while Load Cases F, G, and H were selected because the load truck was in close proximity to the three girders that maintained both internal and external instrumentation through the depth of the beams, and thus yielded the most relevant results pertaining to the composite behavior of the HCB. The transition from positive strain at the tension steel to negative strain within the deck defined the location of the neutral axis, i.e. zero strain. The occurrence of the neutral axis varied for each of the load cases and it was difficult to define a consistent neutral axis location because the profile through the depth was not linear as might be expected for the design assumption of full composite action. As an example, the tensile strains in the arch section of Girder 5 exceeded those in the tensile strand level. At first

it was surmised that the higher concentrations of strain were due to service load tensile cracking in the unreinforced arch concrete, solely intended for support during construction (Van Nossdall et al. 2013). However, after evaluation of the quarter-span strain profiles (Figure 27 - Figure 30), it appears that the two steel strands resting along the bottom of the arch profile, which were used to anchor the stirrups, may be carry significant levels of tension, despite their absence in design calculations. The VWG arch strains seen in the quarter-span plots (Figure 27) are in tension, well beyond the cracking strain of the arch concrete, yet the arch continues to carry the strain. Another potential source of this discrepancy in the neutral axis location is the occurrence of slip between the concrete deck and the HCBs; however, this phenomenon could not be discerned from the available data.

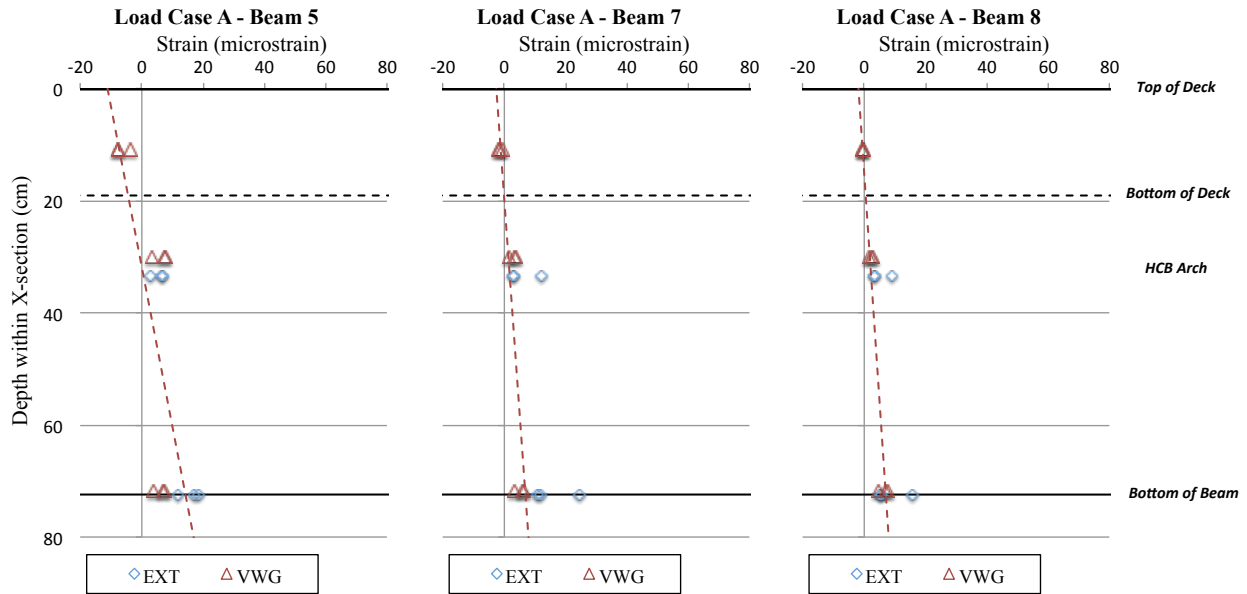


Figure 23 – Midspan Strain Profiles Load Case A

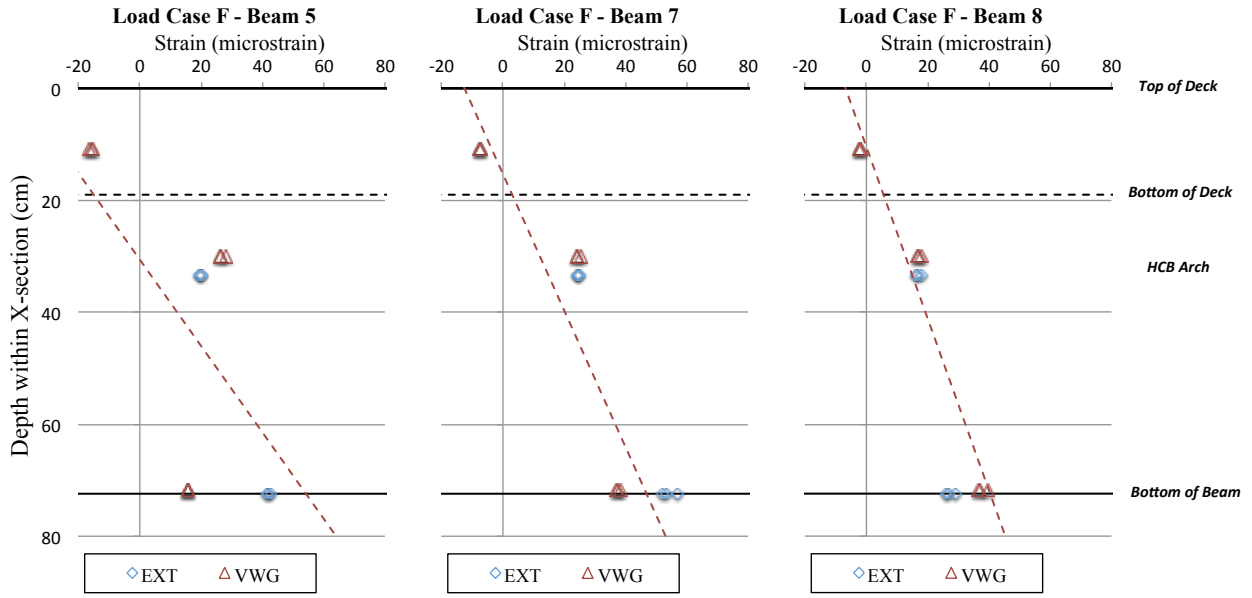


Figure 24 - Midspan Strain Profiles Load Case F

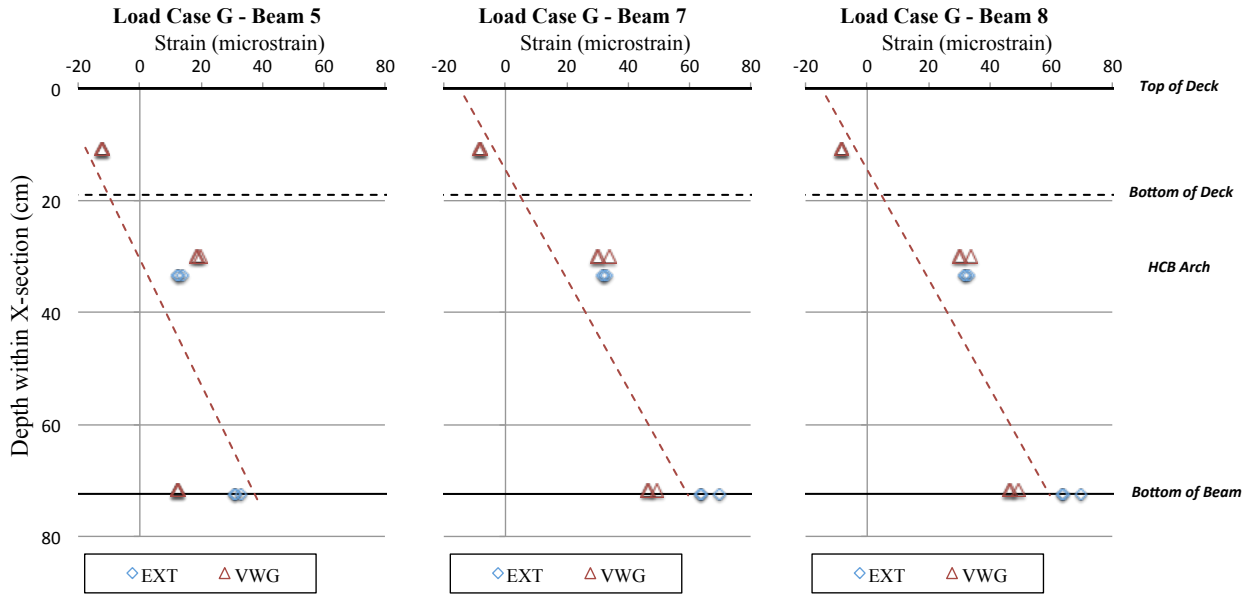


Figure 25 - Midspan Strain Profiles Load Case G

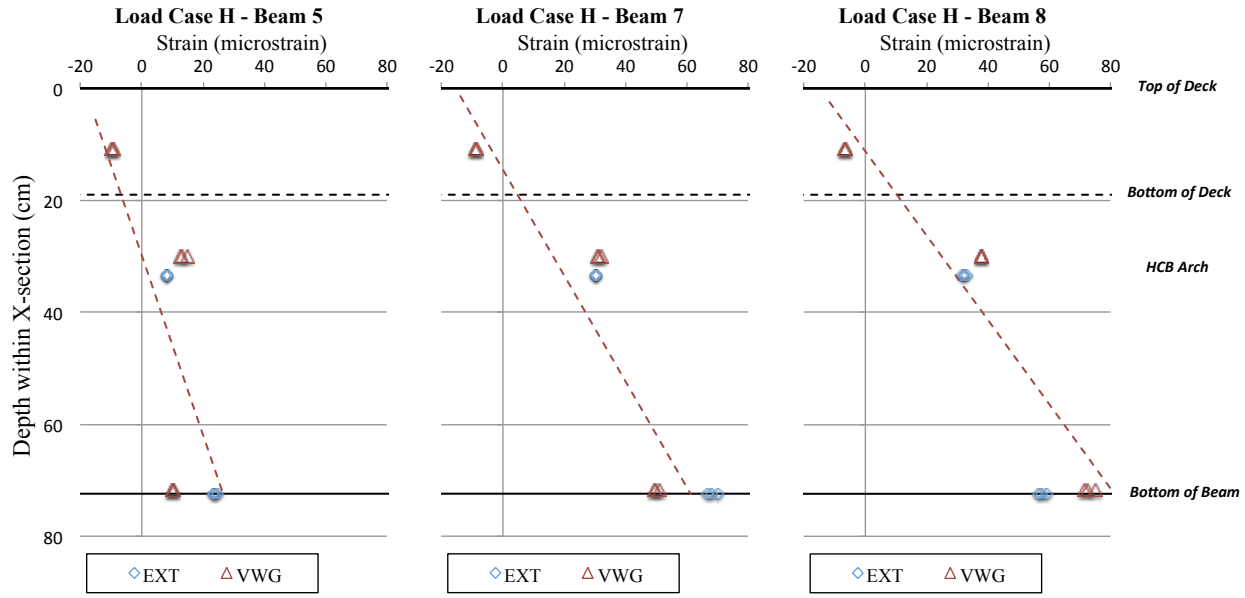


Figure 26 - Midspan Strain Profiles Load Case H

Rather than cracking in the arch, Ahsan (2012) hypothesized that there exists a local bending phenomenon within the concrete arch. As illustrated in Figure 2, it can be rationalized that the arch would be able to experience bending, especially at higher levels of overall HCB curvature where the arch begins to flatten out. Ahsan also proposed that this effect is dampened at mid-span due to the 8 ft sheet of FRP that serves as the bottom formwork for the arch, which also likely provides stiffening to the arch. This FRP sheet that forms an enclosure for the arch at this location also connects to either FRP web and thus enforces greater congruence with the FRP curvature and overall HCB response at mid-span. The data collected in this experimental program aligned with the hypothesis, as the quarter-span arch gauges of Beams 5 and 7 experienced uncharacteristically high levels of tensile strain, often greater than the maximum tensile strain in the bottom flange of mid-span girders. Beam 8 did not exhibit such an accentuated trend, but this was likely caused by the stiffening effect of the parapet in combination with the additional steel (nearly double that in the interior girders) added to the tension zone of the exterior girders. These exterior beams were likely stiff enough to minimize beam curvature, and the local bending effects in the arch were therefore not as evident.

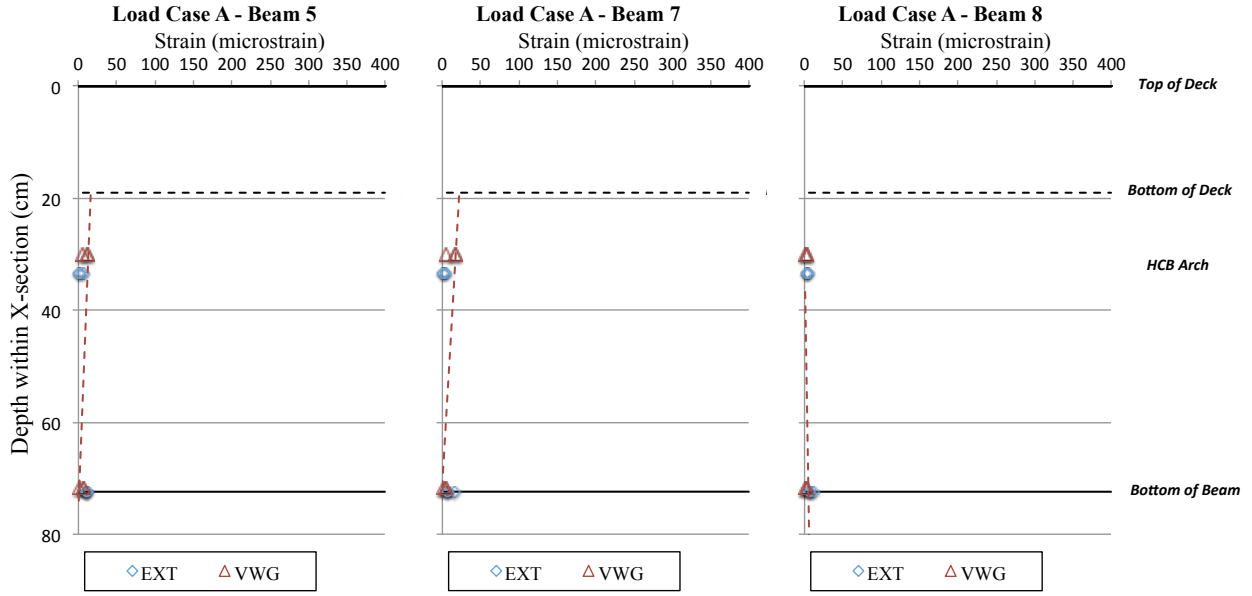


Figure 27 - Quarterspan Strain Profiles Load Case A

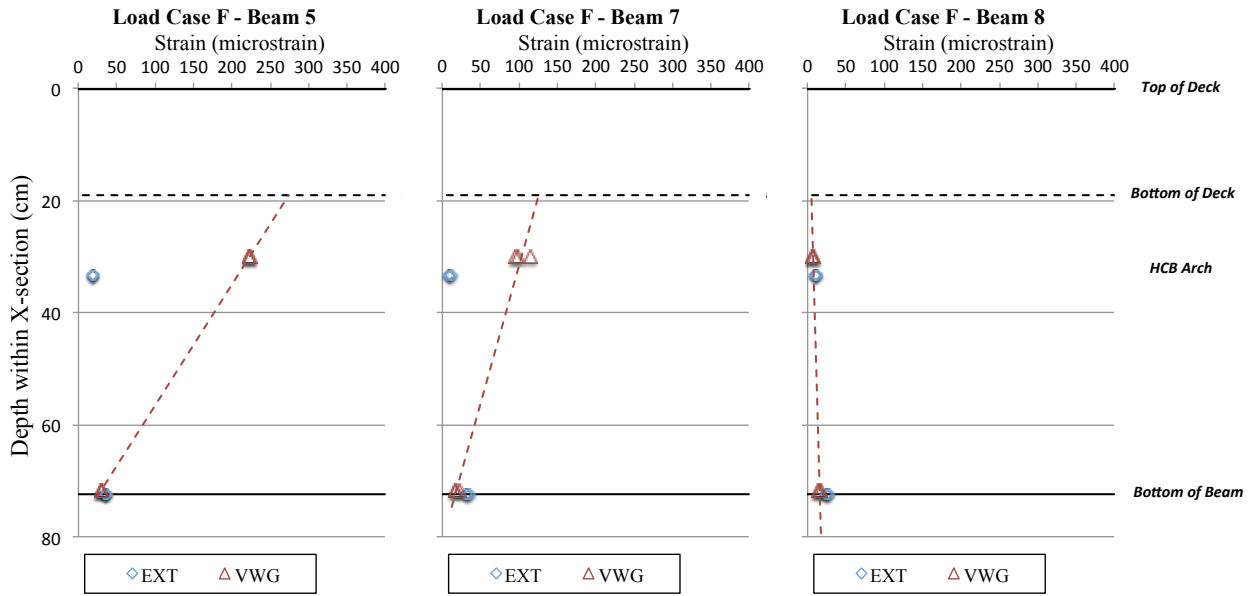


Figure 28 - Quarterspan Strain Profiles Load Case F

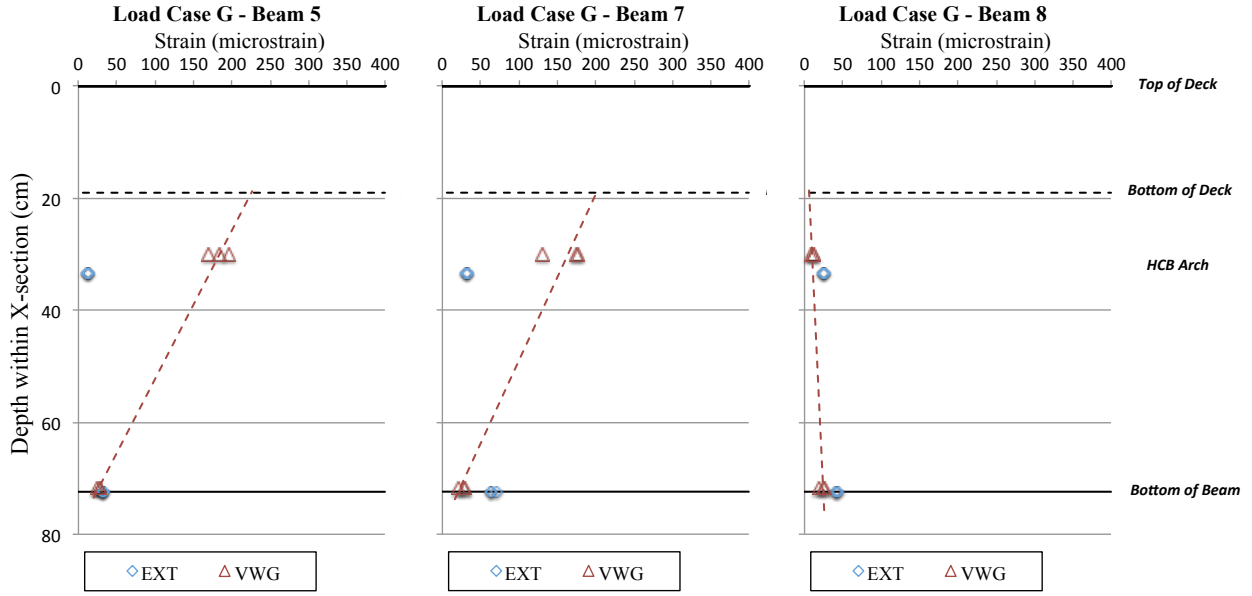


Figure 29 - Quarterspan Strain Profiles Load Case G

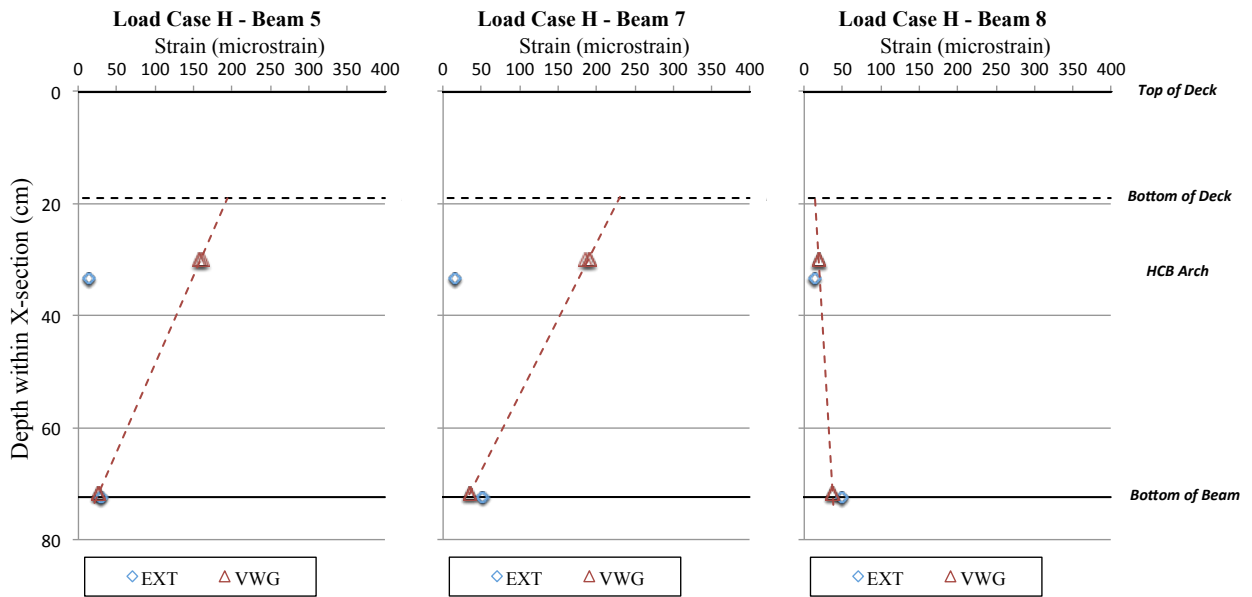


Figure 30 - Quarterspan Strain Profiles Load Case H

Dynamic Load Allowance

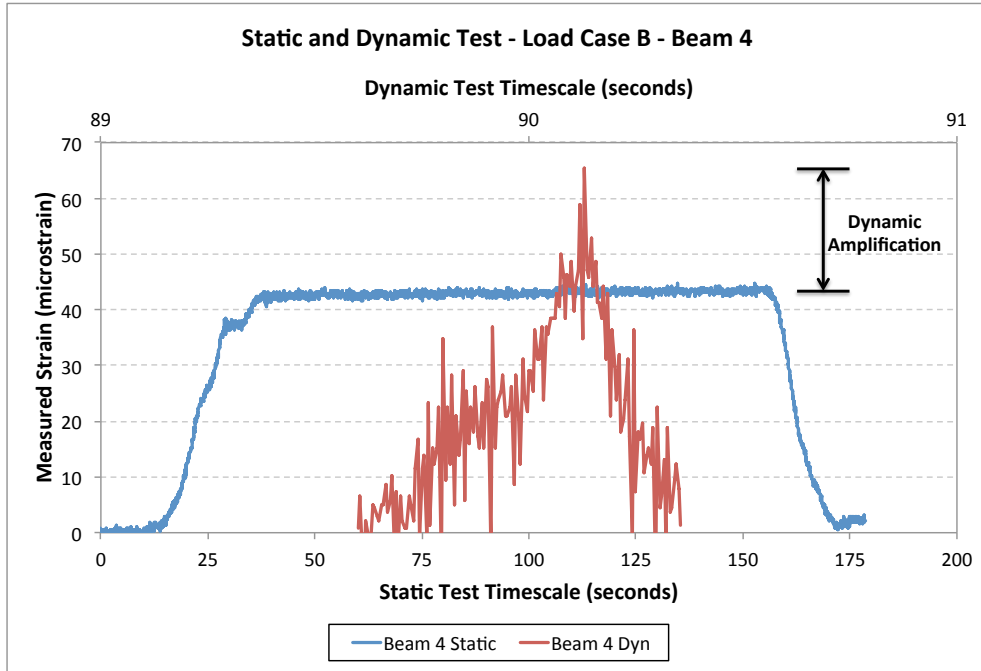
As described in a previous section, the dynamic load allowance (DLA) or impact factor accounts for the amplification of the design static live load due to a moving vehicle crossing a bridge. The dynamic response of HCB was of particular interest in this investigation because of the lightweight of a typical HCB versus a conventional steel or concrete beam. In addition, the design of this system was controlled by deflection and the dynamic response can be related to the inherent flexibility of the system.

To study this behavior, load test results from a static load case and a series of corresponding dynamic load tests were used to determine the dynamic load allowance. As described in the experimental program, the testing was limited to Load Cases B and D to allow the loading truck to traverse the structure near the posted speed limit. Using the relationship presented in Equation 2, the dynamic load allowance, represented as a percent increase, was determined as the additional response observed under dynamic loading conditions relative to the corresponding static response. A representation of this additional dynamic response is presented in Figure 39 from the superposition of strains observed during the static and dynamic tests. All of the measurements for the dynamic response were derived from the externally mounted BDI gauges on the tension side of the HCB beams. The original test plan included plans to measure the VWGs dynamically; however, this effort proved unsuccessful, so only the external gauge measurements were recorded and used in this analysis.

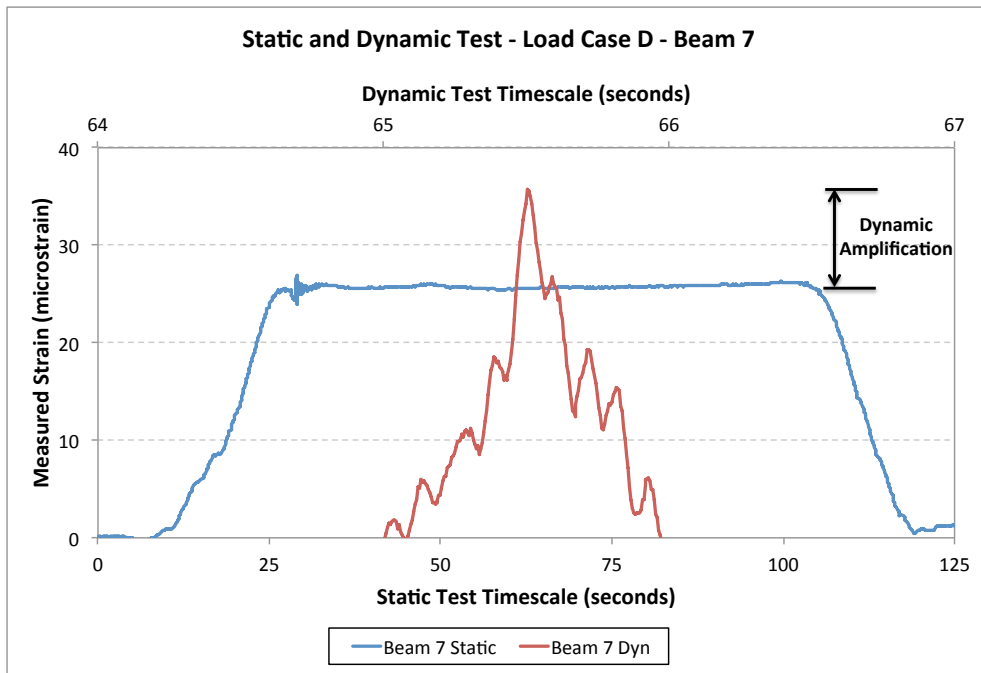
$$DLA = \frac{\epsilon_{\text{dynamic}} - \epsilon_{\text{static}}}{\epsilon_{\text{static}}} \cdot 100\%$$

Equation 2

The controlling or maximum dynamic amplification response for each of the two load truck positions tested under dynamic conditions is presented in Table 4 along with the design values from the AASHTO LRFD and Standard Specification (AASHTO 2002; AASHTO 2012). These measured values represent the amplification observed in the most heavily loaded girders for the respective load cases. The table shows that the average dynamic amplification was comparable to those prescribed by AASHTO, but there is the potential for larger amplification as demonstrated by the maximum responses observed in the most heavily loaded girders, as much as 46% compared to the AASHTO LRFD value of 33%. In the maximum dynamic amplification cases shown, the maximum response registered in Beam 4 for Load Case B was 46%, while a response of 33% was registered in Beam 7 for load case D.



(a)



(b)

Figure 31 - Maximum Dynamic Amplification Response (a) Load Case B and (b) Load Case D

Table 4 – Summary of Dynamic Load Allowance

	Max. DLA	Girder with max response
Load Case B		
Run B1 – Tested at 35 mph	46%	<i>Beam 4</i>
Run B2 – Tested at 40 mph	43%	<i>Beam 4</i>
Load Case D		
Run D1 – Tested at 40 mph	31%	<i>Beam 7</i>
Run D2 – Tested at 45 mph	33%	<i>Beam 7</i>
<i>Measured Average</i>	23%	-
AASHTO		
LRFD	33%	-
Standard Specification	30%	-

FINDINGS AND CONCLUSIONS

The findings of the study may be summarized as follows:

- *Flexural load distribution behavior determined from the externally mounted strain gauges was consistent with expected trends.* The highest strains were registered directly under the load vehicle, and dissipated further away for the point of load application. The controlling experimental distribution factors confirmed Ahsan’s (2012) laboratory work, and similarly yielded distribution factors comparable to those derived for design of typical beam type bridges. For the interior girders, the controlling distribution factor exceeded the AASHTO distribution factor for the Type B (closed steel or concrete box with a concrete deck) category by ~15%, but all other measured distribution factors were lower than the design estimates.
 - It is anticipated that if the HCB system is used in an unballasted track railroad application, this distribution would be similar to that observed during the live load testing. This assumption is based on the premise that the design would be stiffened to accommodate the higher loads and that within the elastic range load distribution behavior can be scaled accordingly. If the system utilized a ballasted deck these findings would not necessarily hold, but it is anticipated that the distribution would likely be more uniform as the ballast would serve to distribute the load more uniformly amongst all of the beams.
 - In addition, the parapet walls of the Tides Mill Stream Bridge offered a significant stiffening contribution to the fascia or exterior girders, which may or may not be present in a railroad bridge because bridges do not typically maintain stiff parapets. A similar observation was made in a study by Otter and Doe (2009), which was attributed to stiffening provided by the ballast curbs. If additional stiffening of the HCB system is required for railroad applications or there was the need for a pedestrian crossing, the addition of stiff parapets could be integrated into the design to minimize demand on the members, especially for members that are further away from the center of gravity of the track.

- While the impact of potential damage mechanisms (impact, section/strand loss) was not investigated in this study, the lateral load distribution response of the HCB system does provide an indication of the similarity to existing bridge designs and the potential for redistribution in the presence of damage. However, this topic warrants further investigation and is a topic of investigation of another NURail project by John Ma – University of Tennessee Knoxville - “Lateral Impact of Railroad Bridges with Hybrid Composite Beams (HCB)”.
- *The typical dynamic load allowance registered was comparable to the AASHTO design values typical for conventional bridge systems, but for some cases the HCB system exceeded this design value.* Several instances of larger amplifications (44-46%) were observed for Load Case B, which positioned the loading vehicle over the second and third most northern girders, indicating that the system may be more compliant than a traditional beam bridge, but additional evaluation may be necessary.
 - For railroad applications, this dynamic response may be a challenge for this system due to the inherent flexibility in the system coupled with the higher impact design loads recommended by AREMA, relative to highway applications. This inherent flexibility can be accommodated in design through increased section or system stiffness (deeper sections, more closely spaced girders, increased tension reinforcement), but this topic warrants further investigation.
- *The FRP shell does not act compositely with the internal HCB components (concrete arch and prestressed strand tie).* The internal strain profiles confirm the assumed neutral axis, but showed a non-linear trend through the depth. It was shown that the arch does not act compositely with the system and the assumption that plane sections remain plane is not valid for HCB. In fact, the arch may exhibit local flexural bending within the girder that is especially apparent at the quarter-spans, but subdued at mid-span due to an additional FRP shell layer beneath the arch that provides additional stiffness.
- *There was also an observed disparity between the bottom flange strains and the strains in the tension steel.* This phenomenon could be explained by slippage of the steel within the FRP flange, though this occurrence has not been experimentally verified. Another way to look at this phenomenon is debonding of the top layer of FRP due to the vertical force applied by the steel during flexure. If the steel were to separate from the outer layers of FRP, there exists insufficient vertical restraint to enforce curvature in the steel during bending, and thus the steel would experience the pure tensile strain associated with a tied arch. The FRP shell would experience the curvature of the deck through the rigidity of the FRP webs and also higher strains than the steel.
 - For railroad application, it should be noted that when the HCB system is designed as a composite system (i.e. HCB beams acting composite with a deck) this phenomena would not be expected to be a major concern considering that primary tensile resistance is provided by the tension

reinforcement once the system is made composite. In this scenario, the HCB beam is primarily in tension under service loads. The scenario with the HCBs not designed compositely with the deck was not included in this investigation, but may warrant further consideration.

- *The shear response of the system was not captured from the experimental program and could not be evaluated based on the research results.*

The research investigation described in this report focused on characterizing the in-service structural behavior of the Hybrid Composite Beam bridge system. Based on the results presented the following conclusions were drawn:

- *The lateral load distribution can be accommodated by existing provisions of the AASHTO LRFD Bridge Design Specifications, if the bridge is described as beam (Case A) or box (Case B) type structure per AASHTO LRFD Bridge Design Specification – Table 4.6.2.2.1-1 (AASHTO 2012). While this provision is not specifically intended for railroad applications, the load distribution characteristics are expected to scale accordingly with appropriately designed HCB members.*
- *The dynamic load allowance or dynamic amplification observed from the live-load testing program was inconsistent when compared against the AASHTO LRFD Bridge Design Specifications (AASHTO 2012) and warrants further investigation.*
- *The element level load sharing response observed from the live-load testing program demonstrated that composite action exists between the HCB and the reinforced concrete deck, but a potential loss of composite action may be present within the HCB element.*

RECOMMENDATIONS

- The HCB bridge system evaluated as part of this investigation highlighted the viability of the system in a traditional bridge application. Coupled with the positive results observed in previous studies, the railroad industry should consider this system further for additional applications that include moderate to short span and applications that require accelerated construction. However, prior to adoption, additional evaluation of the non-composite internal system behavior should be performed to determine if the system is effective for railroad specific serviceability criteria. In addition, consideration should be given to the apparent dynamic response of this lightweight system to determine if serviceability criteria are exceeded for this type of system.
- Future studies on this system should extend the findings to evaluate the performance of this system under different geometries and subjected to railroad specific loadings. It is anticipated that the behavior characteristics will remain the same if the designs are modified to accommodate these loads, but theorized local phenomena such as local arch bending and strand/shell separation may be more prominent at these higher loads.

References

- Ahsan, S. (2012). *Evaluation of Hybrid-Composite Beam for Use in Tide Mill Bridge*. Masters of Science, Virginia Tech.
- American Association of State Highway and Transportation Officials (AASHTO) (2002). *Standard Specification for Highway Bridges*. Washington D.C., AASHTO.
- American Association of State Highway and Transportation Officials (AASHTO) (2012). *AASHTO LRFD bridge design specifications. 6th ed. (with 2013 interim revisions)*. Washington, D.C., American Association of State Highway and Transportation Officials. **2 v. (loose-leaf) :: 1938**.
- Eom, J. and A. Nowak (2001). "Live Load Distribution for Steel Girder Bridges." *Journal of Bridge Engineering* **6**(6): 489-497.
- Harris, D. K. (2010). "Assessment of flexural lateral load distribution methodologies for stringer bridges." *Engineering Structures* **32**(11): 3443-3451.
- Harris, D. K., T. Cousins, T. M. Murray and E. D. Sotelino (2008). "Field Investigation of a Sandwich Plate System bridge deck." *ASCE Journal of Performance of Constructed Facilities* **22**(5): 1-11.
- Hillman, J. R. (2003). *Investigation of a Hybrid-Composite Beam System*. Transportation Research Board. Washington, D.C., IDEA Program Final Report HSR-23.
- Hillman, J. R. (2008). *Product Application of a Hybrid-Composite Beam System*. Transportation Research Board. Washington, D.C., IDEA Program Final Report HSR-43.
- Hillman, J. R. and D. Otter (2008). *Testing of a Prototype Hybrid-Composite Beam Span under Railroad Loadings*. AREAM Annual Technical Conference, Salt Lake City, UT, American Railway Engineering and Maintenance-of-Way Association.
- Otter, D. and B. Doe (2009). *Testing of a Prototype Hybrid-Composite Beam Span at FAST*. Secondary Testing of a Prototype Hybrid-Composite Beam Span at FAST. Secondary Otter, D. and B. Doe. Pueblo, CO.
- Otter, D. and L. Tunna (2011). *Secondary Generation Hybrid Composite Beam Span: Preliminary Assessment at Facility of Accelerated Service Testing*. Secondary Secondary Generation Hybrid Composite Beam Span: Preliminary Assessment at Facility of Accelerated Service Testing. Secondary Otter, D. and L. Tunna. Pueblo, CO.
- Snape, T. and R. Lindyberg (2009). *Test Results: HC Beam for the Knickerbocker Bridge*. Secondary Test Results: HC Beam for the Knickerbocker Bridge. Secondary Snape, T. and R. Lindyberg. Orono, ME.
- Van Nosedall, S., C. D. Moen, T. E. Cousins and C. L. Roberts-Wollmann (2013). "Experiments on a Hybrid-Composite Beam for Bridge Applications." *Transportation Research Record: Journal of the Transportation Research Board* **2332**(1): 43-52.
- Waldron, C. J., T. E. Cousins, A. J. Nassar and J. P. Gomez (2005). "Demonstration of use of high-performance lightweight concrete in bridge superstructure in Virginia." *Journal of Performance of Constructed Facilities* **19**(2): 146-154.